AD_____

Award Number: W81XWH-11-1-0386

TITLE: Targeting Cancer Protein Profiles with Split-Enzyme Reporter Fragments to Achieve Chemical Resolution for Molecular Imaging

PRINCIPAL INVESTIGATOR: Ann-Marie Broome, Ph.D., M.B.A.

CONTRACTING ORGANIZATION: Medical University of South Carolina
Charleston, SC 29425-8908

REPORT DATE: November 2014

TYPE OF REPORT: Final Report

PREPARED FOR: U.S. Army Medical Research and Materiel Command
Fort Detrick, Maryland 21702-5012

REPORT DOCUMENTATION PAGE

Form Approved
OMB No. 0704-0188

1. REPORT DATE	2. REPORT TYPE	3. DATES COVERED
November 2014	Final Report	15 Jul 2011 - 31 Aug 2014

4. TITLE AND SUBTITLE
Targeting Cancer Protein Profiles with Split-Enzyme Reporter Fragments to Achieve Chemical Resolution for Molecular Imaging

5a. CONTRACT NUMBER

5b. GRANT NUMBER
W81XWH-11-1-0386

5c. PROGRAM ELEMENT NUMBER

6. AUTHOR(S)
Ann-Marie Broome, Ph.D., M.B.A.

E-Mail: broomea@musc.edu

5d. PROJECT NUMBER

5e. TASK NUMBER

5f. WORK UNIT NUMBER

7. PERFORMING ORGANIZATION NAME(S) AND ADDRESS(ES)

Medical University of South Carolina
179 Ashley Ave
Charleston, SC 29425-8908

8. PERFORMING ORGANIZATION REPORT NUMBER

9. SPONSORING / MONITORING AGENCY NAME(S) AND ADDRESS(ES)
U.S. Army Medical Research and Materiel Command
Fort Detrick, Maryland 21702-5012

10. SPONSOR/MONITOR'S ACRONYM(S)

11. SPONSOR/MONITOR'S REPORT NUMBER(S)

12. DISTRIBUTION / AVAILABILITY STATEMENT
Approved for Public Release; Distribution Unlimited

13. SUPPLEMENTARY NOTES

14. ABSTRACT

Mutational events that drive a normal cell to become a cancer cell require the coordinated overexpression of multiple biomarkers. Unique biomarker combinations can create dynamic, physiologic patterns at different stages of cancer development. The assignment of protein expression patterns, or protein profiling, to delineate differences between normal tissues and developing cancer is gaining momentum as a critical instrument in aiding diagnosis, tailoring therapeutics, and predicting clinical outcomes. These proteomic studies, however, investigate changes in protein expression in cell lines and bulk tissue specimens at the gross proteomic level. While powerful, this technique fails to account for the heterogeneity of most tumors since the histopathology associated with many cancers encompasses only a small fraction of the total number of cells present in a tissue section. To date, it is impossible to visualize these cancer biomarker patterns *in situ*, which define the status of the cell, both non-invasively and *in vivo*.

We present a major leap in cancer imaging ideology to develop a novel molecular imaging paradigm that utilizes multiple cellular targets to generate imageable signals in the same cell thereby achieving chemical resolution. *The objective of our proposed research is to develop a new imaging platform consisting of targeted-trans-complementing reporter fragments to simultaneously image the cancer signature in vivo and in real time.* A number of unique advantages of this imaging platform are envisaged, such as: 1) increased specificity; 2) multi-marker imaging at the cellular level; and 3) ability to recognize distinct genetic patterns among different tumor types and grades. In the proposed experiments, we will conjugate each reporter fragment to one of two different ligands to simultaneously target and image *in vivo*, via enzyme reporter re-construction *in situ*, a molecular signature consisting of two or more different targets. If the cells contain only one or none of the targets, no reporter signal will be observed. The feasibility of this imaging paradigm will be conducted *in vivo* with animals bearing tumors that express either a subset or all of the biomarkers required for enzyme *trans*-complementation.

15. SUBJECT TERMS molecular imaging, enzyme complementation, cancer biomarkers, epidermal growth factor receptor					
16. SECURITY CLASSIFICATION OF: U			17. LIMITATION OF ABSTRACT	18. NUMBER OF PAGES	19a. NAME OF RESPONSIBLE PERSON USAMRMC
a. REPORT U	b. ABSTRACT U	c. THIS PAGE U	UU	34	19b. TELEPHONE NUMBER *(include area code)*

TABLE OF CONTENTS

INTRODUCTION

Targeted-reporter platforms answer a critical unmet need and have real application for imaging the multi-step progression of cancer growth that requires the coordinated overexpression of multiple biomarkers. The development of these platforms to investigate molecular signatures associated with disease creates the next frontier in *in vivo* imaging. The importance for imaging molecular signatures is underscored by the almost weekly publication of sets of genomic markers that are diagnostic or predictive of disease states. By exploiting multi-marker imaging, we ultimately seek to image combinations of biomarkers that will uniquely identify cancers from normal tissue and report on the biochemical status of cancer cells. These expression patterns can thus be indicative of the type, stage, or severity of disease. However, the application of imaging molecular signatures is far more expansive than just applications for cancer diagnosis or disease detection. Once developed, we will be able to transform molecular imaging from single biomarker identification to imaging and interrogating cellular dynamics during other complex processes such as embryonic development, growth, proliferation, and differentiation in addition to cellular changes that occur early in the course of disease.

Our research seeks to utilize relatively innocuous building blocks to create an exquisitely intuitive platform. By linking a reporter fragment to a targeting moiety, we are only constrained by the number of fragments with which the reporter can be cleaved. The underlying hypothesis of this work is: *trans*-complementing subunits of image-able enzymes can be exploited to design a system so that multiple changes in a cancer cell's diagnostic signature can be imaged simultaneously. This approach is only achievable by utilizing subunit complementation, which provides a chemical resolution that is far more precise than the physical or anatomical-based resolution currently employed to produce data using non-invasive imaging hardware. The pioneering utility of the technique significantly increases specificity, decreases background artifacts, and promotes our ability to interrogate the status of cells rather than just the presence of cancer biomarkers. Thus, by expanding the number of biomarkers available to non-invasive diagnostic and therapeutic assessment, we envision an innovative platform-based approach to disease identification, staging, and treatment.

BODY

Our research aims to utilize inactive subunits of an image-able enzyme that are added exogenously to the targeted cells or tissue via intravenous injection into the animal. No tinkering with the genome of the diseased tissue is required and these bio-probes can be utilized to report on the physiologic expression levels of important biomarkers in any tissue to which they are administered. The development of such a non-invasive imaging system that bases disease detection on biochemical differences rather than on anatomical differences between normal and diseased tissues is clearly innovative and provides an intelligent-design strategy to pursue non-invasive assessment of diagnostic and prognostic genetic signatures *in vivo.* Eventually, this technology will have the ability to accurately assess the entire mass of a diseased tissue rather than a limited biopsy of the tissue, providing a more comprehensive knowledge of genetic changes than either individual genetic or proteomic analyses can achieve.

To develop an epidermal growth factor receptor (EGFR) targeted imaging complex that would cross the Blood Brain Barrier (BBB) and selectively bind to brain tumor cells overexpressing EGFR, we created a peptide-based near infrared (NIRF) probe to compare to full-length EGF. This allowed us to assay specificity, kinetic behavior, and binding affinity of the receptor-targeted peptides as outlined in ***Specific Aim 1 Milestone 1***. For these studies, we employed a peptide discovered through phage display screening against purified human EGFR. The peptide was modified to include linkers and a NIRF dye (**Fig. 1**). To determine the optimal space between the NIRF dye and the peptide, we designed and synthesized a series of peptides to include increasing numbers of discrete ethylene glycol units to serve as linkers between a Cy5.5 and the N-terminal end of the peptide. Cy5.5 and EGF_{pep} were either directly linked or linked via 1, 2, or 3 units of discrete ethylene glycol (AEEA) moieties (**Fig. 1**). To determine which of the compounds optimally interacts with cells

expressing EGFR, the apparent binding for each bioconjugate was fluorometrically determined from a saturation binding assay in vitro using a human GBM cell line overexpressing EGFR, Gli36Δ5, (**Table 1**). Compounds 1, 2, 3, and 4 all bound to the cells with affinities in the micromolar (μM) range. Compound 2, which had a single linker, had the highest apparent affinity with a Kd at least 2-fold better than compound 1, which had no ethylene linker, 8.9 μM to 18.5 μM respectively. Compounds 3 and 4 have significantly higher affinities for binding, 64.4 μM and 123.0 μM, respectively.

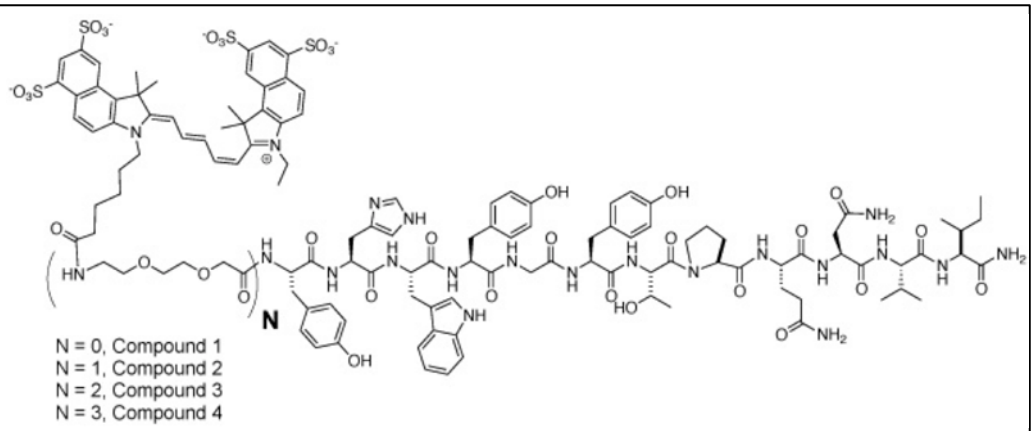

Fig. 1. EGFR-binding peptides (EGF_{pep}). EGF_{pep} is conjugated to a near-infrared fluorophore, Cy5.5, linked with up to three units of amino-ethoxy-ethoxy-acid (AEEA) at the N-terminal amine of the peptide.

Compound	Peptide (EGF_{pep})	K_d (μM)
1	Cy5.5- YHWYGYTPQNVI-amide	18.5 ± 3.9
2	Cy5.5-$(AEEA)_1$-YHWYGYTPQNVI-amide	8.9 ± 3.7
3	Cy5.5-$(AEEA)_2$-YHWYGYTPQNVI-amide	64.4 ± 24.6
4	Cy5.5-$(AEEA)_3$-YHWYGYTPQNVI-amide	123.0 ± 174.0
5	YHWYGYTPQNVI-amide (GE11-amide)	ND
6	Cy5.5-$(AEEA)_1$-NYQTPVYGWIYH-amide (scrambled)	ND

Table 1. Binding affinities of the EGF peptides.

We next used immunofluorescence microscopy to determine the fate of the peptide complexes once they bound to glioblastoma cells expressing EGFR. As predicted from the affinity measurements, compound 2, which had the highest affinity, also showed the greatest accumulation of fluorescence after incubation with Gli36Δ5 cells (**Fig. 2A**). Neither compound 1 (no linker) nor either of the molecules with greater linker numbers (compounds 3 and 4) was taken up by the cells to the same extent as compound 2.

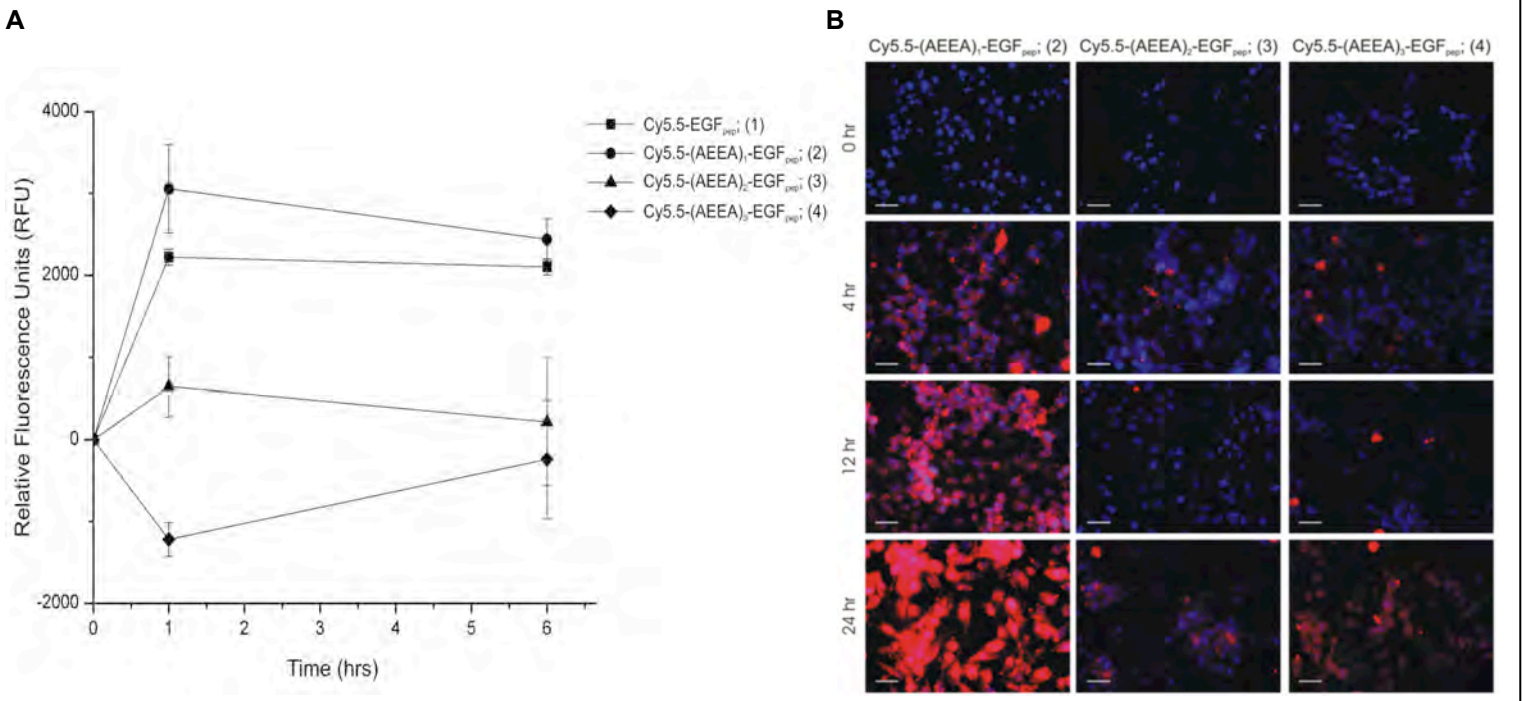

Fig. 2. *In vitro* studies of the peptides with different linker lengths. **A**, Gli36Δ5 cells were incubated with 1 μM of compound 2 [Cy5.5-$(AEEA)_1$-EGF_{pep}] and the cell associated fluorescence was measured using spectrofluorometry at the indicated times. **B**, Cells were incubated with 1 μM compounds over time. Uptake of the compounds was assessed using epi-fluorescence microscopy. Representative images are shown. Images = 40X magnification. Scale bar = 50 μm.

Interestingly, cells took up the peptide with the longest linker and the worst binding affinity, compound 4, better than compound 3 (**Fig. 2B**). Compound 4 compares most closely to commercially available full-length EGF by linker numbers; however, the presence of the hydrophilic Cy5.5 fluorophore appears to impact binding affinity. When tested against U87-MG cells, which express much lower levels of the EGFR (**Fig. 4A**), no cellular uptake for any of the compounds was observed (**Fig. 3**).

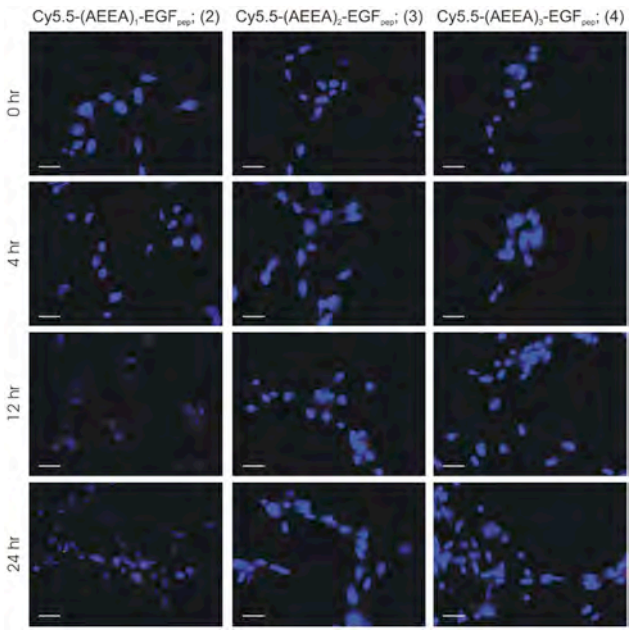

Fig. 3. No accumulation of peptides in cells lacking wild-type EGFR. U87-MG cells were incubated with 1 μM compounds for the indicated times. Uptake of the compounds was assessed using epi-fluorescence microscopy. Representative images are shown. Images = 40X magnification. Scale bar = 50 μm.

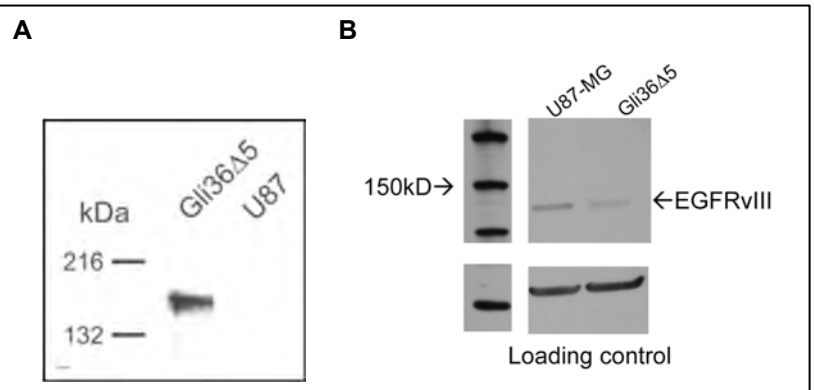

Fig. 4. Differential expression levels of EGFR and EGFRvIII. **A**, Relative levels of wild type EGFR expressed in Gli36Δ5 and U87-MG glioblastoma cell lysates using an antibody specific to wild type EGFR. **B**, Mutant EGFRvIII content in in Gli36Δ5 and U87-MG tumor cells lines using an EGFRvIII specific antibody. β-actin was used as a loading

Since we wanted to specifically target wild-type EGFR and not mutant derivatives, such as the EGFRvIII, often found in cancer and a different cancer cell lines, we also examined the expression of EGFRvIII in various cell lines. Western blots for the EGFRvIII on both U87-MG and Gli36Δ5 cells showed that the mutant receptor expression is similar (**Fig. 4B**) for both cell lines. In addition, saturation binding studies conducted with A431 cells, a squamous carcinoma cell line, that expresses high levels of only wild type EGFR (**Fig. 5A**), indicated that the

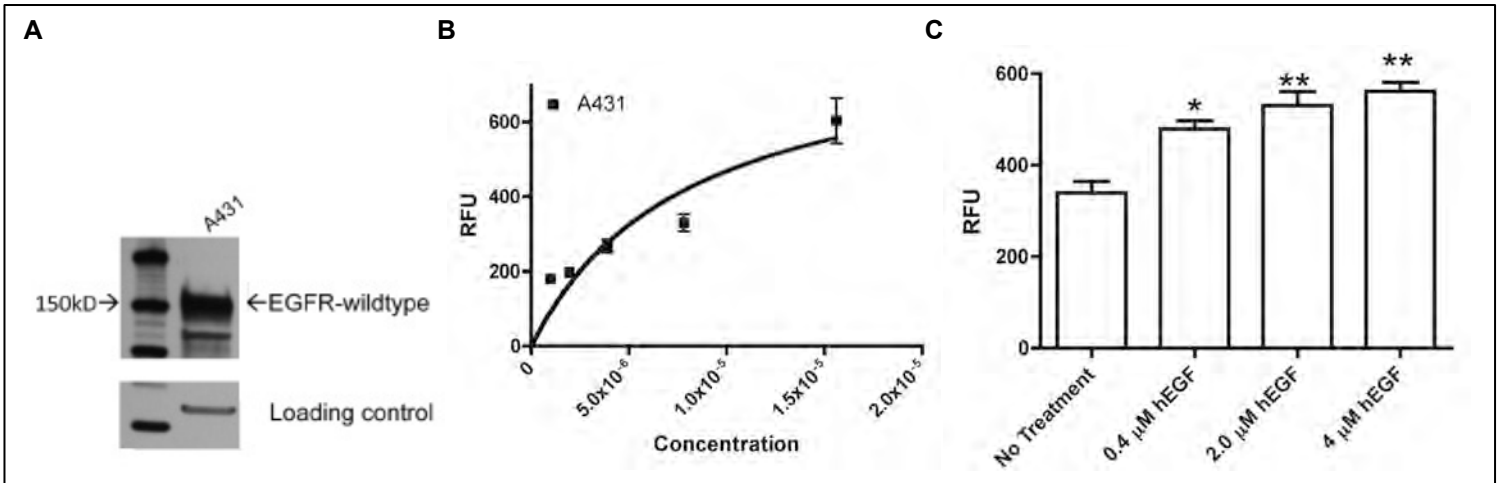

Fig. 5. A, Expression levels of the wild type EGFR determined by Western blot in the A431 cell lines. Loading control was determined by blotting against β-actin. **B**, Saturation binding assay. Compound **2** was incubated with A431 cells at increasing concentrations for 1 hour, washed, and cell associated Cy5.5 was quantified. The Kd determined for the A431 cell line was 8.0±3.0 μM. **C**, Cell uptake of compound **2** in the presence of hEGF ligand. A431 cells were plated in 96-well plates and were treated with 1 μM of Cy5.5-EGFpep in the presence of increasing amounts of hEGF (or no treatment) for 90 minutes. Uptake increased with increasing EGF stimulation. These data suggest that uptake of labeled ligand is specific to EGF receptors. *, P>0.01; **, P>001.

Kd for binding was similar to that measured with Gli36Δ5 cells (**Fig. 5B**). Further, incubation of compound **2** with A431 cells displayed increasing fluorescence in the presence of the EGF ligand, which increases cycling of wild type EGFR in cells (**Fig. 5C**).

Consequently, we were able to determine the optimal peptide length and degree of functionalization of each linker length. We were also able to create NIR-conjugated peptides that targeted with variable receptor affinities and demonstrated that the linker length affected uptake and accumulation using the wild type EGFR specifically. These results were prepared as a manuscript and published in *Molecular Cancer Therapeutics* (2012) **11**(10): 2202-11 (please see ***Appendix A***).

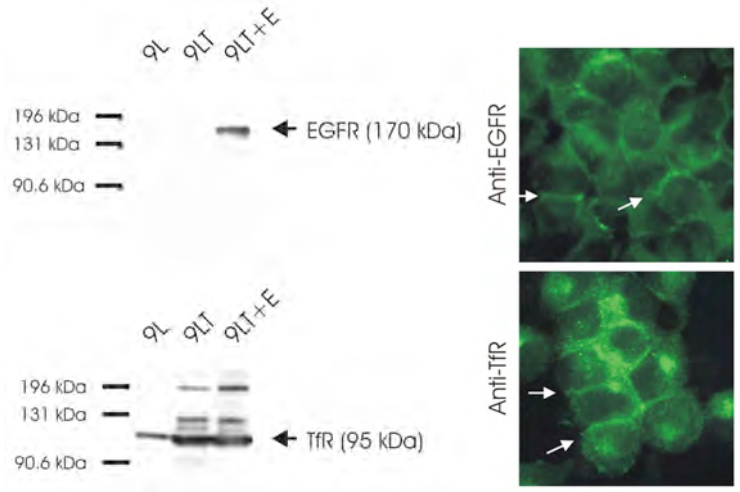

Fig. 6. Genetically engineered rat glioma, 9L, cell lines overexpressing EGFR and TfR. **A**, Western blot analysis of cell lines overexpressing none (9L), one (9LT) or two (9LT+E) human cell surface receptors. **B**, The overexpressed receptors are localized to the cell membrane (white arrows) and within the cytoplasm after staining with either anti-EGFR or anti-TfR.

During the time period covered in this progress report, we were able to characterize a series of engineered *in vitro* cancer signature glioma cell lines as outlined in ***Specific Aim 1 Milestone 3***. Rat glioma cells (9L) were stably transfected with pcDNA3.1 plasmids containing the full length coding region of the human EGFR or the human transferrin receptor (TfR). To create a cell line overexpressing both receptors, 9L cells overexpressing TfR were stably transfected with pcDNA3.1-EGFR and selected using antibiotics. Western blotting was used to show the relative expression of each human receptor protein in engineered cell lines (**Fig. 6A**). Immunofluorescence staining localizes the receptors both at the cell membrane (arrows) and within the cytoplasm of the cells (**Fig. 6B**). We also examined the expression of EGFR and TfR in the human glioma cell lines, Gli36Δ5 and U87, described in detail above.

To prepare the β-galactosidase (β-gal) complexes, we linked biotinylated EGF for the EGFR to biotinylated β-gal using fluorophore-conjugated streptavidin. Ligand, linker, and reporter fragment were mixed in a molar ratio 1:1:3 at room temperature for 1 hr. Excess D-biotin was added to block any remaining unbound streptavidin sites. In the case of control assays, untargeted reporter complex was prepared with D-biotin, in place of the ligand, mixed with linker and reporter fragment in a molar ration 1:1:3.

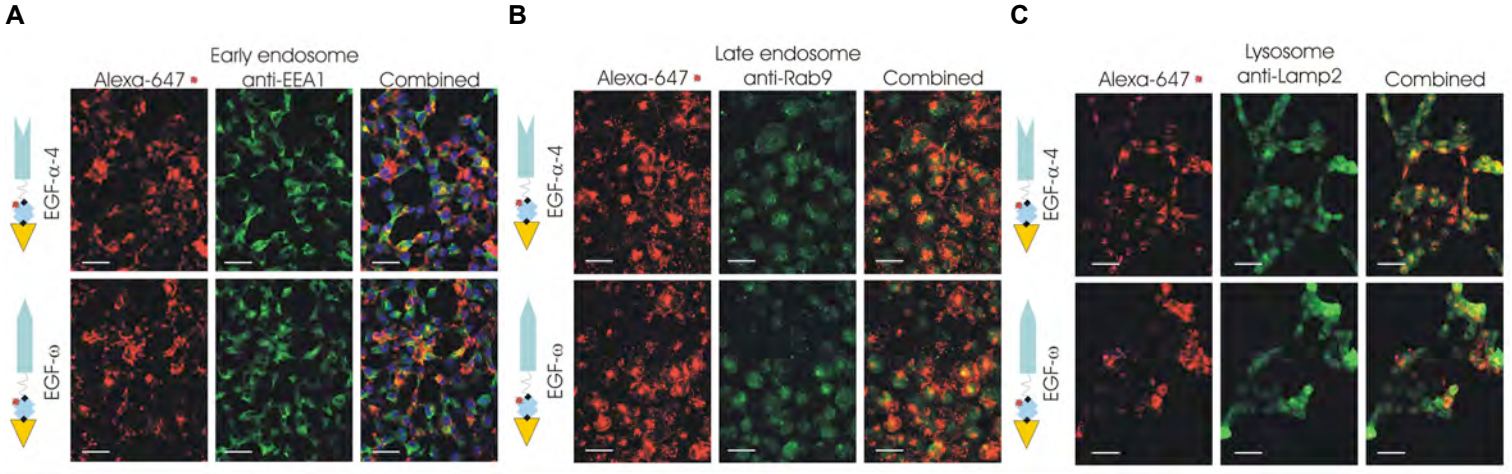

Fig. 7. EGFR-targeted split-β-galactosidase pairs co-localize in vesicles in the endosomal pathway. Gli36Δ5 cells were incubated with EGF ligand-complex (1 nMole) for 1 hr at 37 °C. The cells were then fixed with 4% paraformaldehyde, rinsed with PBS, and blocked with 1% host serum for 30 min at room temperature. Coverslips were incubated with primary antibody against EEA1 (**A**), Rab9 (**B**), or Lamp-2 (**C**) at room temperature for 2 hrs. The cells were counterstained with DAPI to visualize the nuclei, mounted, and observed using confocal microscopy. Images = 40X magnification. Scale bar = 50 μm.

In our studies, complementation of the β-gal subunits involves a multiplicity of molecules; thus, tracking the uptake and accumulation of each single targeted-complex is necessary to evaluate the bioavailibilty of the imaging agents as outlined in ***Specific Aim 1 Milestone 4***. We used fluorescence microscopy to follow the spatial and temporal distributions of targeted-β-galactosidase subunits during internalization of the target, EGFR. Full-length EGF, the targeting moiety, was linked to either the α-4 subunit (EGF-α-4) or ω subunit (EGF-ω) of β-gal. Human glioblastoma cells, Gli36Δ5, overexpressing the EGFR were incubated for 4 hrs at 37 °C with each complex singly. An intrinsic fluorophore conjugated to the linker allowed us to examine the sub-cellular localization of each targeted-complex. As expected, cells that overexpress the EGFR bind and take up the EGF-targeted β-gal subunits. The targeted-complexes can be found throughout the functional EGFR internalization pathway, primarily in early endosomes (**Fig. 7A**) and lysosomes (**Fig. 7C**). Very little of either EGF-targeted complex was found in late endosomal vesicles (**Figure 7B**). Addition of the EGFR-targeted complexes did not adversely affect the viability of the cells as assayed by trypan blue staining (**not shown**).

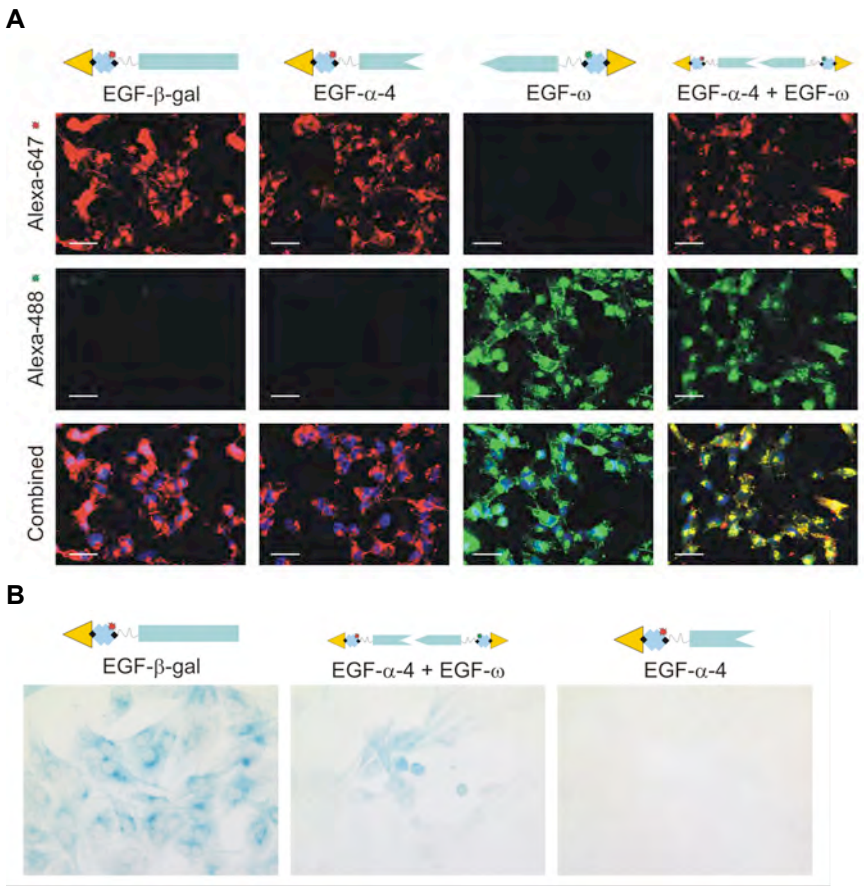

Fig. 8. *In vitro* complementation of targeted split-β-galactosidase pairs. **A**, Immunofluorescence of Gli36Δ5 cells incubated with full length β-gal or complementing pairs of β-gal subunits. Co-localization is seen by overlay of red and green to produce yellow. **B**, Cells incubated with either targeted-full length β-gal or complementing pairs retained enzymatic activity as seen after X-gal staining. Images = 40X magnification. Scale bar = 50 μm.

Next, we examined whether concomitant incubation of cells with both targeted β-gal subunits altered either the uptake or location of the targeted-complexes (**Fig. 8A**). Gli36Δ5 cells were incubated for 4 hrs at 37 °C with EGF-β-gal, EGF-α-4 singly, EGF-ω singly, or the combination of EGF-α-4 and EGF-ω. In this case, the EGF-α-4 complex was labeled with Alexa 647 fluorophore and the EGF-ω complex was labeled with Alexa 488 fluorophore to distinguish between the two complexes. EGFR-targeted α-4 and ω complexes each sequestered in a manner similar to that of targeted-full length β-gal. The combination of both targeted-complexes did not negatively impact the uptake of either complex. The targeted-complexes co-localized to the same location predominately, although EGF-α-4 was observed in disparate locations approximately 20% of the time as measured by relative fluorescence densitometry. Enzymatic activity was visualized by overnight X-gal staining (**Fig. 8B**).

Incubation of EGF-α-4 or EGF-ω with its non-targeted, complementing partner, i.e. B-ω or B-α-4, respectively, further demonstrated the specificity of the targeting moiety to drive the uptake and accumulation of the complex (**Fig. 9**). Non-targeted complementing fragments were not internalized as shown by a lack of intrinsic florescent signal; also, the presence of the non-targeted fragment did not inhibit the uptake of the targeted-complex. As a final control, uptake specificity of EGF-α-4 or EGF-ω was competitively inhibited in the presence

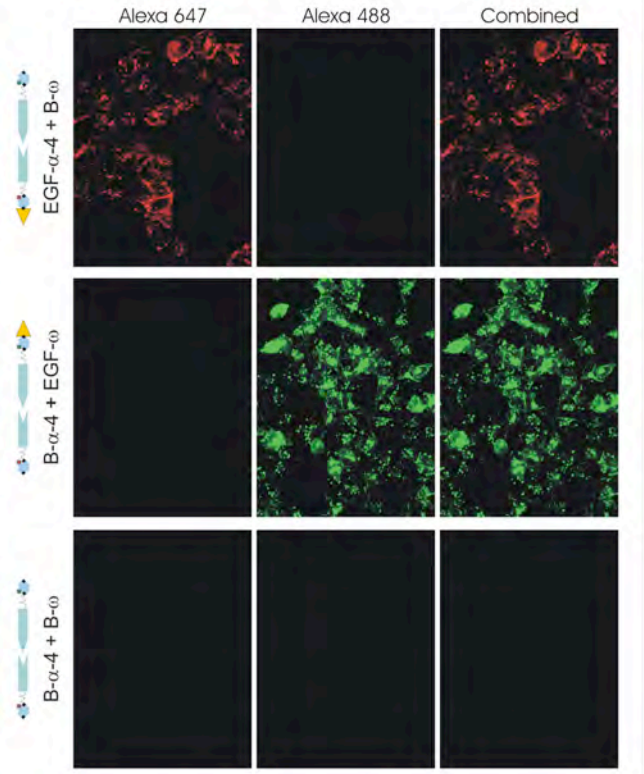

Fig. 9. Non-targeted β-galactosidase fragments do not accumulate within the cells. Gli36Δ5 cells incubated with 1 nM targeted-subunit simultaneously with the non-targeted complementing subunit for 1 hr at 37C only accumulated the targeted-subunit as observed by confocal microscopy. Images = 40X magnification.

of increasing concentrations of free EGF ligand (**Fig. 10**). Uptake of EGF-α-4 is dramatically decreased with both a 1:1 (200 nM) and 1:5 (1000 nM) ratio of complex to free ligand as visualized by fluorescence microscopy (**Fig. 10A**). EGF-ω is also inhibited, but not to the same extent as EGF-α-4. The relative fluorescence of each treatment regime was quantified and graphed. EGF-α-4 binding was reduced by 68% at the highest concentration of free ligand and EGF-ω was reduced by approximately 40% (**Fig. 10B**).

Several different combinations of complementing pairs of β-gal were examined for uptake and enzymatic activity as proposed in ***Specific Aim 1 Milestone 5***. The most robust pair to date is the α-4 and ω combination. The α-4 and 1-ω pair also demonstrated relatively strong enzymatic activity, but staining took longer the optimal 18 hrs. The only inefficient pair was the α-1 and 1-ω pair. This is not unexpected since the α-1 fragment is very small and rapidly diffuses away, out of the cellular compartments were complementation could be optimized. In the short term, we will move forward into *in vivo* studies with the α-4 and ω complementing pair.

We next tested the utility of the construct to accumulate in tumors expressing EGFR using an orthotopic mouse model for brain tumors. Glioma cells,

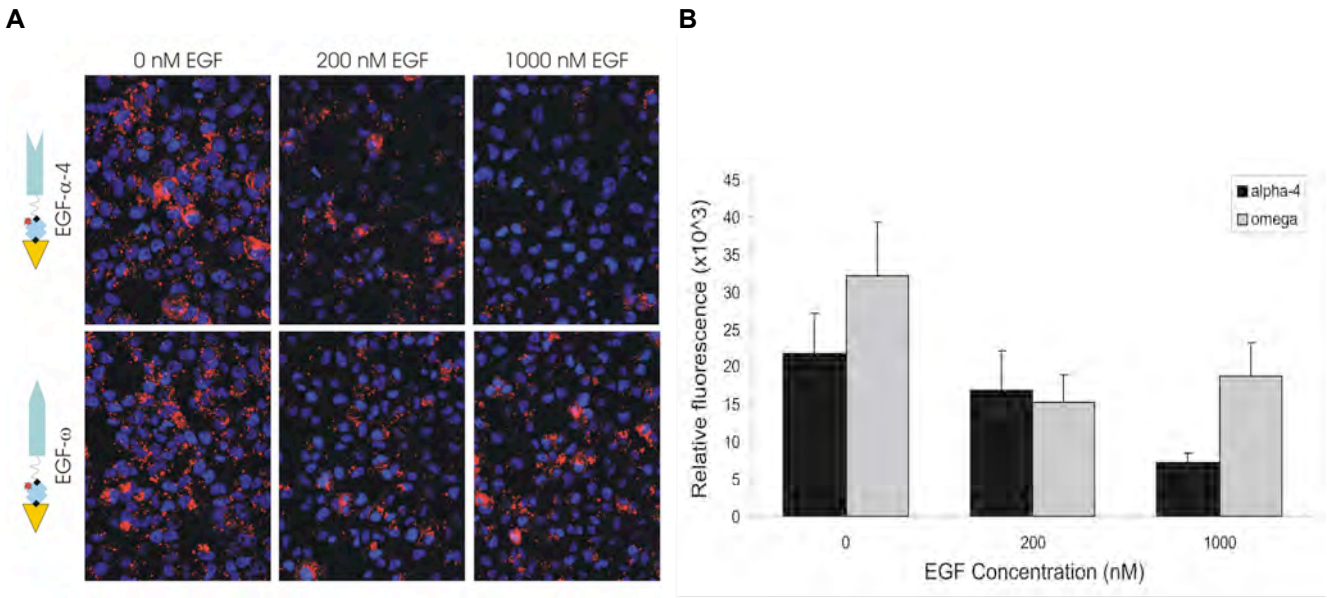

Fig. 10. Targeted β-galactosidase fragment uptake is specific for the EGF receptor. Gli36Δ5 cells were incubated with 1 nM targeted-subunit simultaneously with increasing concentrations of free EGF for 1 hr inhibited uptake of the targeted complex. Fluorescence was quantified and graphed to demonstrate the reduction in complex binding. Images = 40X magnification.

Gli36Δ5, were stereotactically implanted in the brains of mice and grown for approximately 10 days as per IUCAC approved protocols (***Specific Aim 2 Milestone 2***). Mice were intravenously injected with 1 mg/kg body weight of either EGF-β-gal (targeted) or B-β-gal (non-targeted), both of which incorporated Alexafluor 647-labeled streptavidin to easily visualize targeted-complex uptake following tissue preparation (**Fig. 11A**). Targeted-β-gal crossed the BBB as measured by fluorescence molecular tomography in living mice (**Fig. 11B**). Approximately 3-5% (~133 nM) of the injected dose accumulated within the tumor within 4 hours. After 4 hours, the mice were euthanized and the brains were removed and imaged whole and then serially transected into 2 mm sections and imaged again *ex vivo* using an *in vivo* Maestro fluorescence imaging system (**Fig. 11C**, top panels). EGF-β-gal specifically accumulates in the tumor within 4 hours. In contrast, non-targeted B-β-gal did not accumulate in the tumor as indicated by a lack of fluorescent signal, but presumably remained in the ventral cerebral and cerebellar arteries of the brain (**Fig. 11C**, bottom panels).

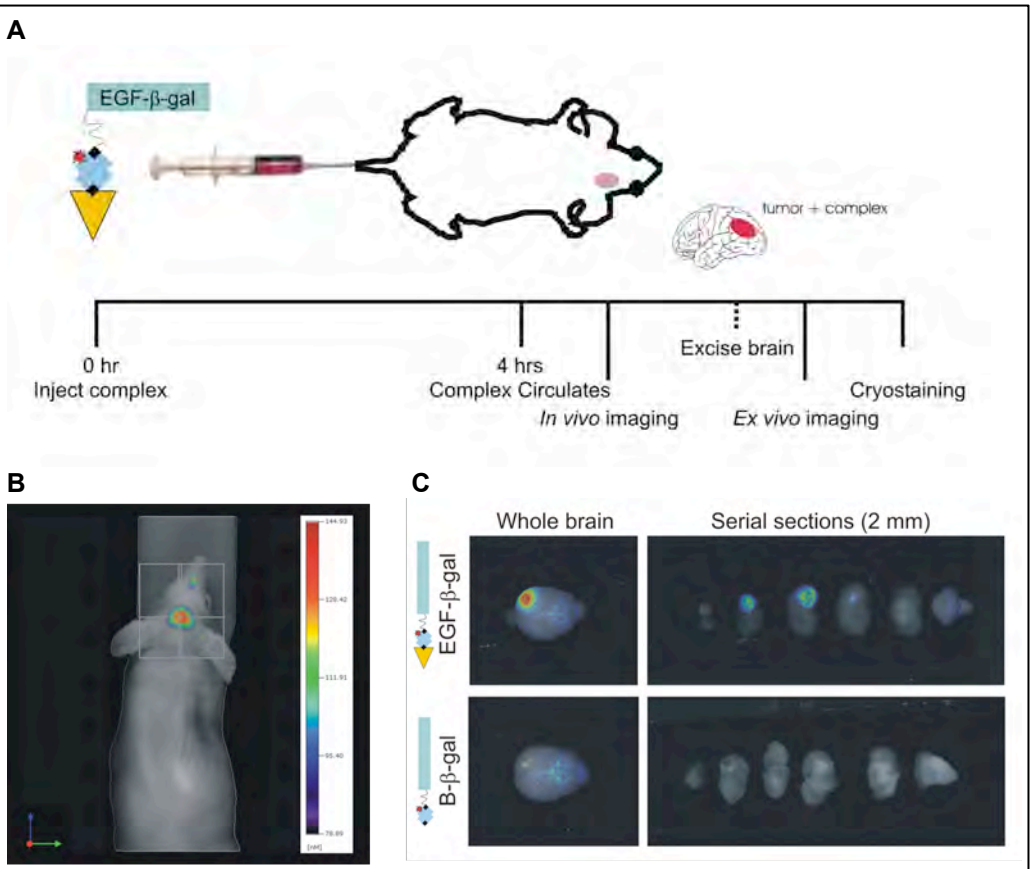

Fig. 11. Fluorescence imaging of targeted-β-galactosidase complex in orthotopic brain tumors. Gli36Δ5 cells were implanted in mice and injected with either EGF-β-gal or B-β-gal.

Serial sections of the brains were cryosectioned and counterstained with DAPI to delineate cell nuclei. Fluorescence images captured at 100X magnification clearly showed significant EGF-β-gal uptake within the tumor and internalization within the cells'

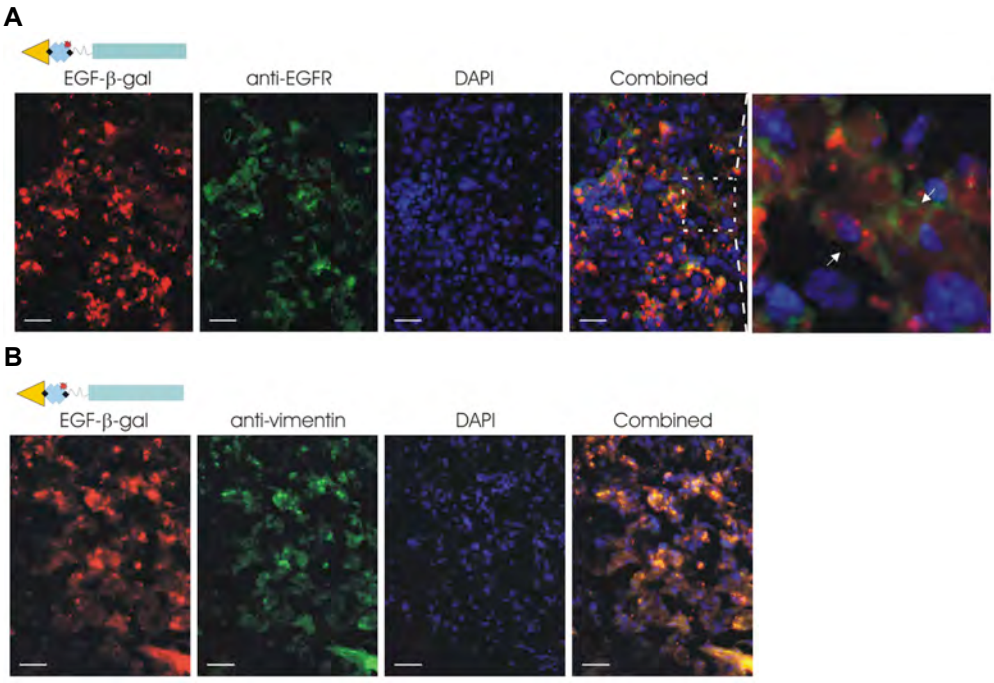

Fig. 12. Validation of targeted-β-galactosidase complex in orthotopic brain tumors.

cytoplasm. Cryosections of brain containing the tumor region were then counterstained with anti-EGFR (**Fig. 12A**) or anti-vimentin (**Fig. 12B**) and visualized using epi-fluorescence microscopy. These studies indicated that EGFR is heterogeneously expressed within the tumor (green) and that targeted-β-gal complex (red) accumulates specifically in glioma cells overexpressing EGFR (**Fig. 12A**). Vimentin staining, a standard pro-invasive intermediate filament tumor marker, identified implanted cells within the orthotopic mouse model which were of human origin, i.e. Gli36Δ5 cells, and demonstrated that targeted-β-gal complex (red) only co-localized within human cells expressing vimentin (green) (**Fig. 12B**). Little to no β-gal complex was found within other regions of the brain (data not shown).

We next sought to determine if β-gal activity was maintained by the targeted complex for ***Specific Aim 2 Milestone 3***. For these studies orthotopic brain tumors implanted as described above were used. After approximately 10 days of growth tumors were harvested by removing the intact mouse brain and then sectioning it into 2 mm sections. Following sectioning, a bioluminescent β-gal substrate, Galacton-Plus, was topically applied to the *ex vivo* brain serial sections to evaluate the delivery and integrity of enzyme across the BBB (**Fig. 13A**). Further, this targeting ability and enzymatic activity in Gli36Δ5-derived brain tumors, expressing high levels of EGFR, was compared to brain tumors implanted with U87 cells expressing low levels of EGFR. Robust bioluminescence was captured within the tumor overexpressing EGFR after 3 minutes, indicating that β-gal maintained its activity. Minimal β-gal activity was observed in U87-derived tumors, which express very low levels of the EGFR protein as previously determined by Western blot. The luminescence was quantified and Gli36Δ5 tumors possessed 3-4-fold more enzymatic activity than U87 tumors (**Fig. 13B**). Tumor cryosections counterstained with EGFR antibody (green) and DAPI (blue) demonstrated the differences in both the level of EGFR expression and EGFR-targeted uptake of the β-gal complex within the two tumor types, high EGFR expression and low EGFR expression, respectively (**Fig. 13C**). Western blot analysis confirmed the higher expression levels of EGFR observed in Gli36Δ5 cells versus U87 cells.

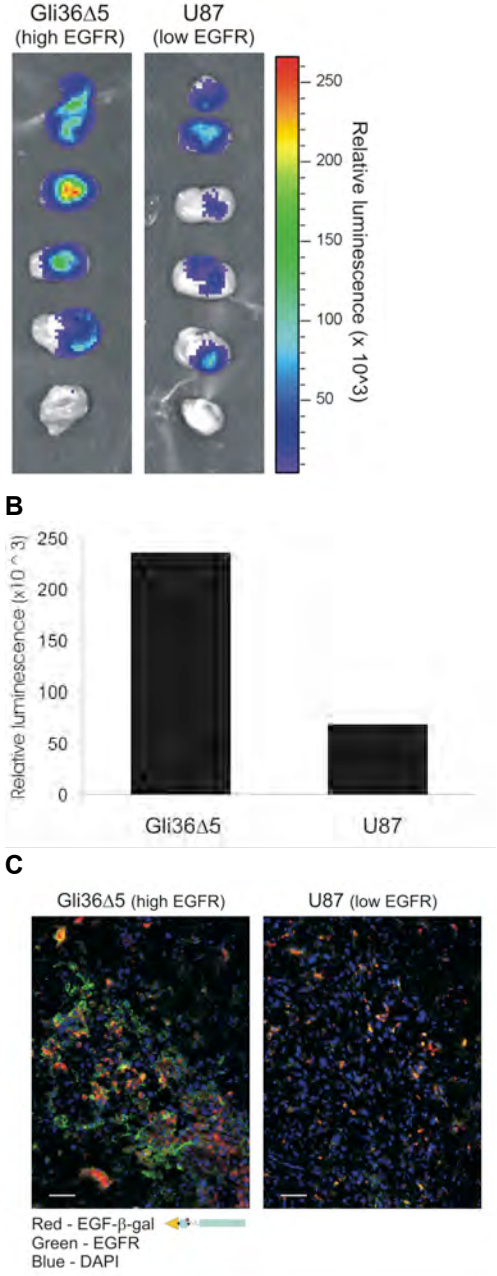

Fig. 13. *Ex vivo* bioluminescence imaging of targeted-β-galactosidase complex.

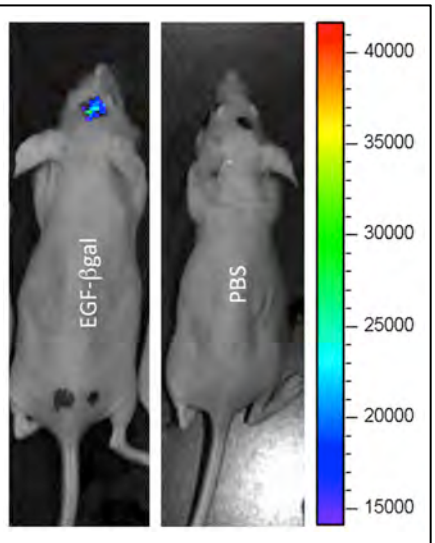

Fig. 14. Non-invasive imaging of targeted-β-galactosidase complex in orthotopic brain tumors.

The next step in these studies was to demonstrate that complex formation could be imaged *in vivo* in living mice as outlined in ***Specific Aim 3 Milestone 1***. Mice containing orthotopically-implanted Gli36Δ5 cells were intravenously injected with 1 mg/ kg body weight of EGF-β-gal, (**Fig. 14**). Four hours later, Galacton-Plus, bioluminescence β-gal substrate, was stereotactically injected into the brain cavity through the original burr-

hole used to implant the tumors. Targeted-β-gal crossed the BBB as measured by bioluminescence imaging in living mice. Little to no bioluminescence was observed in sham treated mice. These results were prepared as a manuscript and published in *Bioconjugate Chemistry* (2015) **26**(4): 660-8. (please see ***Appendix B***).

KEY RESEARCH ACCOMPLISHMENTS

The following lists the key research accomplishments emanating from this research during this grant:

- Synthesis of NIRF-EGF peptide probe (EGF-Cy5.5) with high affinity for the EGFR and specific accumulation in cells overexpressing EGFR.
- Demonstration that mutant EGFR, EGFRvIII, is not required to effectively image cancer cells *in vitro*.
- Characterization of linker length on uptake and accumulation of EGF-Cy5.5 using kinetic dissociation assay and immunofluorescence microscopy.
- Creation of genetically engineered rat glioma cell lines overexpressing no human receptors, one human receptor, or combination of two human receptors.
- Evaluation of EGFR and TfR pattern of overexpression in human glioma cell lines, Gli36Δ5 and U87.
- Self-assembly of targeted β-gal complexes.
- Track uptake and accumulation of EGFR targeted-complex into the endosomal pathway.
- *In vitro* complementation of targeted split-β-galactosidase pairs.
- Recognition that the optimal complementing β-gal pairs, α-4 and ω, are the most robust pair to move forward into *in vivo* animal tumor model studies.
- *In vivo* imaging of EGFR targeted-complex in orthotopic mouse model of brain tumor.
- *Ex vivo* validation of EGFR targeted-complex uptake in orthotopic mouse model of brain tumor corresponds with upregulated EGFR expression.
- *Ex vivo* imaging of EGFR targeted-complex in orthotopic mouse model of brain tumor using bioluminescence.

REPORTABLE OUTCOMES

Original research papers:

Agnes, R.S.; Broome, A-M.; Kavik, K.; Verma, A.; Wang, J.; & Basilion, J.P. (2012) An optical probe for noninvasive molecular imaging of orthotopic brain tumors overexpressing epidermal growth factor receptor. *Molecular Cancer Therapeutics*. **11**(10): 2202-11. [PMCID: PMC3829608] Impact factor: 5.23

Broome, A-M.*; Ramamurthy, G.; Lavik, K.; Liggett, A.; Kinstlinger, I.; & Basilion. J.P.* (2015) Optical imaging of targeted beta-galactosidase in brain tumors to detect EGFR levels. *Bioconjugate Chemistry*. (*corresponding author) 26(4): 660-8. [PMID: 25775241] Impact factor: 4.821

Invited lectures:

- Molecular imaging gets personal: The future of personalized diagnostics and therapeutics. (2011) *Malone University Alpha Gamma Chapter Induction Ceremony*.
- Molecular imaging: The future of personalized medicine. (2011) *CWRU School of Medicine Radiology Grand Rounds*.
- Novel molecular imaging platforms. (2011) *University of Akron Chemistry Seminar Series*.
- Molecular imaging gets personal: targeting the cancer signature. (2011) *MUSC Center for Biomedical Imaging Seminar Series*.
- Imaging the tumor microenvironment with novel bio-molecule constructions. (2011) *Tumor Microenvironment and Metastasis Focus Group.*

- Building targeted-split enzyme nanomolecule complexes using directed self-assembly. (2011) *Foundations of Nanoscience: Self-Assembled Architectures and Devices, 8th Annual Meeting*.
- Molecular imaging gets personal: The future of personalized diagnostics and therapeutics. (2012) *Wayne State University School of Medicine Radiology Grand Rounds*.
- Small animal imaging. (2012) *Medical University of South Carolina Hollings Cancer Center Jenny Sullivan Sanford Melanoma Research Retreat.*
- Exploiting the molecular signature: Enabling unique applications in cancer imaging. (2012) *Medical University of South Carolina Center for Biomedical Imaging Pre-clinical UG Seminar Series.*
- Size does matter in pre-clinical imaging: Challenges and other barriers with brain imaging. (2013) *Perkin Elmer and Sandford Burnham Pre-clinical Imaging Methods Seminar.*
- Overcoming the barriers of theranostic delivery to the brain. (2013) *Clemson University Page Morton Hunter Distinguished Lecture Series*.
- Treating gliomas with nanotechnology-based drug delivery systems (2013) *Medical University of South Carolina Hollings Cancer Center Spring Retreat.*
- Big things come in nano-sized packages: Bridging nanotechnology and molecular imaging. (2013) *Medical University of South Carolina MSTP Seminar Series.*
- Small solutions for big problems: Nanotechnology in an imaging world. (2014) *University of Maryland, Baltimore County Chemistry Seminar Series.*
- SMART nanotechnology for drug delivery in pediatric brain tumors. (2014) *Darby Children's Research Institute Research Day.*
- Image-guided drug delivery in cancer. (2014) *Development Cancer Therapeutics/ CGMR Retreat.*

Oral presentations at international conferences:

- Targeting split-enzyme reporter fragments to achieve chemical resolution for molecular imaging. (2011) *SPIE BiOS: Biomedical Optics Symposium*.
- Optical imaging of targeted beta-galactosidase in brain tumors to detect EGFR levels. (2015) *Nanotech, Microtech, Biotech, Cleantech Joint 2015 Conferences TechConnect World Meeting.*

Poster presentations at international conferences and workshops:

- Verma, A.; Ramamurthy, G., Chung, S.; Broome, A-M.; and Basilion, J.P. (2011) Targeted-enzyme complementation to image cancer receptors. *BMES Annual Meeting*.
- Broome, A-M.; Ramamurthy, G.; Lavik, K.; Verma, A.; & Basilion, J.P. (2011) Targeted-split enzyme nanomolecule complexes for molecular imaging of the coordinated expression of cell surface receptors in glioblastomas. *World Molecular Imaging Congress*. *Best Poster in Category*.
- Agnes, R.S.; Broome, A-M.; & Basilion, J.P. (2011) Differential fluorescence molecular imaging of EGFR in brain tumors. *World Molecular Imaging Congress*.
- Agnes, R.S.; Broome, A-M.; & Basilion, J.P. (2011) Targeted, non-invasive optical imaging agent for fluorescence molecular tomography studies. *American Peptide Society, 22nd American Peptide Symposium*.
- Ramamurthy, G.; Broome, A-M.; Lavik, K.; Verma, A.; & Basilion, J.P. (2011) Imaging the coordinated expression of cell surface receptors in glioblastomas using a novel multi-functional enzyme reporter complementation complex. *American Association for Cancer Research, 102nd Annual Meeting*.
- Broome, A-M.; Ramamurthy, G.; Lavik, K.; Pinter, M.; Kinstlinger, I.; & Basilion, J.P. (2012) Targeted-split enzyme complementation to interrogate the cancer signature using molecular imaging. *World Molecular Imaging Congress*.
- Broome, A-M.; Ramamurthy, G.; Lavik, K.; Verma, A.; Pinter, M.; Basilion, J.P. (2012) Molecular imaging of the cancer signature using targeted-split enzyme complementation. *American Association for Cancer Research, 103rd Annual Meeting.*

Funding applied for:

1R01 CA164368-01 (Multi-PI: **Broome, A-M**) 12/01/2012 - 11/30/2016
NIH Advanced In Vivo Imaging to Understand Cancer Systems (R01) Research Grant
Proteomic Guided In Vivo Molecular Imaging
Role Investigator: Multi-Principal Investigator Total Direct Costs:
Action: Not funded; resubmit

Employment applied for and received based on experience supported by this award:

Associate Professor
Director of Molecular Imaging, Center for Biomedical Imaging
Director of Small Animal Imaging, Hollings Cancer Center
Medical University of South Carolina
Department of Radiology and Radiological Sciences
Center for Biomedical Imaging
Charleston, SC 29425

CONCLUSION

Targeted-reporter platforms have real utility for imaging the multi-step progression of cancer growth that requires the coordinated overexpression of cell surface biomarkers. The development of these platforms to investigate molecular signatures associated with disease creates the next frontier in *in vivo* imaging. The exponential number of genomic marker sets that are considered diagnostic or predictive of disease states underscores the importance of imaging molecular signatures. By exploiting multi-marker imaging, we ultimately seek to image combinations of biomarkers that will uniquely identify cancers from normal tissue and report on the biochemical status of these cells. These expression patterns can thus be indicative of the type, stage, or severity of disease. The application of imaging molecular signatures is therefore critical for cancer and disease detection.

Our research utilizes inactive subunits of an image-able enzyme that are driven to complementation by targeting specific biomarkers on the surface of cells. By linking a reporter fragment to a targeting moiety, this approach provides a cellular resolution that is far more precise than the physical/ anatomical-based resolution currently employed. The pioneering utility of the technique significantly increases specificity, decreases background artifacts, and, combined with a cancer systems approach, promotes our ability to interrogate the status of cells rather than just the presence of cancer biomarkers. In the studies described here, we will utilize a bi-complementation strategy.

Published OnlineFirst July 17, 2012; DOI: 10.1158/1535-7163.MCT-12-0211

APPENDIX A

Molecular Cancer Therapeutics

Preclinical Development

An Optical Probe for Noninvasive Molecular Imaging of Orthotopic Brain Tumors Overexpressing Epidermal Growth Factor Receptor

Richard S. Agnes[1], Ann-Marie Broome[1,2], Jing Wang[1], Anjali Verma[2], Kari Lavik[2], and James P. Basilion[1,2,3]

Abstract

We have developed a near-infrared (NIR) probe that targets cells overexpressing the EGF receptor (EGFR) for imaging glioblastoma brain tumors in live subjects. A peptide specific for the EGFR was modified with various lengths of monodiscrete polyethylene glycol (PEG) units and a NIR Cy5.5 fluorescence dye. The lead compound, compound 2, with one unit of PEG displayed good binding (8.9 μmol/L) and cellular uptake in glioblastoma cells overexpressing EGFR *in vitro*. The *in vivo* studies have shown that the probe was able to selectively label glioblastoma-derived orthotopic brain tumors. *In vivo* image analyses of peptide binding to the tumors using fluorescence-mediated molecular tomography revealed that the compound could distinguish between tumors expressing different levels of EGFR. The data presented here represent the first demonstration of differential quantitation of tumors expressing EGFR in live animals by a targeted NIR fluorescence probe using a molecular imaging device. *Mol Cancer Ther; 11(10); 2202–11. ©2012 AACR.*

Introduction

Glioblastoma multiforme (GBM) is the most common and most malignant of the glial tumors. In 40% to 50% of these tumors, mutations resulting in the overexpression or activation of the EGF receptor (EGFR) are found (1, 2). EGFR is a tyrosine kinase cell surface receptor that regulates growth and survival including adhesion, migration, differentiation, and other cellular processes (3). Thus, the EGFR is considered a validated molecular biomarker for certain cancers including non–small cell lung, head and neck, colorectal, and ovarian cancers.

EGF protein and antibodies to the receptor have both been used to probe for EGFR in tumors. An alternate approach to targeting EGFR is to develop small molecular weight molecules that directly bind to the receptor, including peptide-based entities. Numerous studies suggest that small peptides can efficiently bind to surface receptors (4). One way to identify peptide ligands for protein targets is phage display (5, 6). Using this screening method, randomized libraries of peptides can be generated and screened for affinity and selective molecular targeting to cell surface receptor proteins, such as the transferrin receptor (7, 8). Using phage display techniques, Li has identified a 12-residue linear peptide sequence, GE11 (YHWYGYTPQNVI) approaching nanomolar affinity for EGFR (9). We have used this sequence to develop a fluorescently labeled tumor-selective agent that can cross the blood–brain–tumor barrier (BBTB) and noninvasively interrogate the level of EGFR expression in tumors.

Tremendous interest in the development of noninvasive optical imaging technologies exists for diagnosis of cancer and monitoring of the therapeutic response (10, 11). As optical instrumentation advances (e.g., tomographic imaging), the development of optical imaging molecules that are selective for tumors for *in vivo* studies is fast becoming an important field for cancer research (12). Thus, the ability to differentially image EGFR expression levels might provide noninvasive means to identify tumors that aide in the selection of treatments as well as means of targeted drug delivery.

Specifically, in this work, we synthesized different versions of the imaging agent by varying the length of polyethylene glycol (PEG) linker between the peptide and the fluorochrome, Cy5.5. These imaging compounds were then tested in tissue culture cells lines expressing different levels of the EGFR and in orthotopic brain tumors generated from the cell lines. It was determined that the length of the linker critically affected the efficacy of the agent both in tissue culture and in the *in vivo* setting. Furthermore, these agents were capable of discriminating

Authors' Affiliations: Departments of [1]Radiology and [2]Biomedical Engineering, and [3]NFCR Center for Molecular Imaging, Case Western Reserve University, Cleveland, Ohio

Note: Supplementary data for this article are available at Molecular Cancer Therapeutics Online (http://mct.aacrjournals.org/).

Corresponding Author: James P. Basilion, Departments of Radiology, Biomedical Engineering, and Pathology, NFCR Center for Molecular Imaging at Case, Case Western Reserve University, Wearn Building, Room B-42, 11100 Euclid Avenue, Cleveland, OH 44106. Phone: 216-983-3264; Fax: 216-844-4987; E-mail: jxb206@case.edu

doi: 10.1158/1535-7163.MCT-12-0211

Published OnlineFirst July 17, 2012; DOI: 10.1158/1535-7163.MCT-12-0211

tumors expressing different levels of EGFR in orthotopic GBM models.

Materials and Methods

Probe synthesis and analysis

The peptides were synthesized manually using protocols previously described (13). Peptide was labeled in solution with monoreactive Cy5.5 NHS ester (CyDye, GE Healthcare). Crude fluorophore-labeled peptides were purified by reversed phase high-performance liquid chromatography (RP-HPLC). The isolated peak was lyophilized and characterized matrix-assisted laser desorption/ionization (MALDI) mass spectrometry was done under positive mode. Compounds are characterized by RP-HPLC under 2 different conditions and by thin layer chromatography with 3 different solvent conditions. Details are found in Supplementary Information (Supplementary Tables S1 and S2). Concentration of stock Cy5.5-labeled peptide solutions in dimethyl sulfoxide (DMSO) was determined by UV-Vis spectrometry [Cy5.5 molar extinction coefficient is 250,000 $(mol/L)^{-1}\,cm^{-1}$ at 675 nm; ref. 14].

Cell culture

Human glioblastoma astrocytoma, an epithelial-like cell line U87-MG, and human glioblastoma cell line stably overexpressing the EGFRvIII-mutant form of the *egfr* gene, Gli36Δ5, were used in these studies. U87-MG and A431 cells were recently obtained from American Type Culture Collection. Gli36Δ5 cells were obtained from E.A. Chiocca and were authenticated by Research Animal Diagnostic Laboratory at the University of Missouri (Columbia, MO) for interspecies and mycoplasma contamination by PCR analysis (15). Cell lines were maintained in RPMI or Dulbecco's Modified Eagle's Medium (DMEM; Gibco), respectively, and supplemented with 10% FBS and 1% penicillin–streptomycin. The cells were incubated at 37°C in a humidified 5% CO_2 atmosphere. For Gli36Δ5 cells, puromycin was also included to maintain the expression of the EGFRvIII plasmid.

Saturation binding assays

To determine binding affinities of the Cy5.5-labeled peptides 1 to 4 to EGFR, a saturation binding assay protocol using labeled fluorescence ligand against cell surface receptors was adapted as previously reported (16). Briefly, Gli36Δ5 cells were plated 20,000 cells per well were plated on black Costar 96-well plates (cat. no. 3603). Probes were diluted to range of concentration (0–25 μmol/L) in growing media with 0.3% bovine serum albumin (BSA) and added into wells and incubated at 37°C for 90 minutes at 5% CO_2. Cells were then washed with PBS twice and dried. DMSO was added before reading fluorescence (excitation 670 nm, emission 700 nm) with a Tecan Infinite M200 plate reader. Saturation binding assay data were in quadruplicates and analyzed using one site binding classical equation for nonlinear regression analysis with the GraphPad Prism version 4.0.

Receptor uptake immunofluorescence

Gli36Δ5 or U87-MG cell lines plated in 96-well culture plates (20,000 cells per well; 3 wells per condition) were incubated over indicated time periods with 1 μmol/L of Cy5.5-labeled EGF peptides 2, 3, and 4 at 37°C and 5% CO_2. Cells were briefly rinsed with HEPES buffer and imaged with a Tecan Infinite M200 fluorescence plate reader (excitation 670 nm, emission 700 nm).

Immunocytochemistry of cells grown on coverslips

Gli36Δ5 or U87-MG cancer cell lines were plated on coverslips and incubated overnight to promote adherence. The cells were then fixed with 4% paraformaldehyde, rinsed with PBS, and blocked with 1% host serum for 30 minutes at room temperature. Coverslips were incubated with primary antibody at room temperature for 2 hours. Antibodies used were mouse anti-human wild-type EGFR (1:100 dilution; clone DAK-H1-WT, Dako cat. no. M7289). The coverslips were then rinsed with PBS and counterstained with 4′,6-diamidino-2-phenylindole (DAPI) for 10 minutes at room temperature to visualize the nuclei. After a final rinse with PBS, the coverslips were mounted using Fluor-Mount aqueous media, sealed with nail polish, and observed using epifluorescence microscopy.

Orthotopic brain tumor model

NIH athymic nude female mice (5–8 weeks and 20–25 g upon arrival, NCI-NIH) were maintained at the Animal Resource Center at Case Western Reserve University (Cleveland, OH) according to institutional policies. All procedures were done aseptically according to Institutional Animal Care and Use Committee (IACUC)-approved protocols. Cell for brain implantation were harvested with 1 mL 0.05% trypsin-EDTA (Gibco) and briefly washed with PBS. Trypsin was inactivated by the addition of serum-containing media. The resulting cell suspension was centrifuged at $1,000 \times g$ for 3 minutes. The cell suspension was centrifuged and the supernatant was removed after 2 washes in PBS. Finally, the cells were resuspended in 2 μL PBS for brain implants per animal (250,000 cells per animal for brain implants). Immediately following the cell harvesting procedure, animals were inoculated. For brain tumor implantation, mice were anesthetized by intraperitoneal (i.p.) injection of 50 mg/kg ketamine/xylazine and fitted into a stereotaxic rodent frame (David Kopf Instruments). A small incision was made just lateral to midline to expose bregma suture. A small (1.0 mm) burr hole was drilled at anterior (AP) = +1, lateral (ML) = −2.5 from the bregma. Glioblastoma cells were slowly deposited at a rate of 1 μL/min in the right striatum at a depth of 3 mm from dura with a 10-μL syringe (23-G needle). The needle was slowly withdrawn and the incision was closed with 2 to 3 sutures. Brain tumors grew for 10 to 12 days as per IACUC protocols at which point *in vivo* imaging studies were conducted. As control for the effects of surgical intervention, animals were also subjected to the implantation procedure but

Published OnlineFirst July 17, 2012; DOI: 10.1158/1535-7163.MCT-12-0211

received 2 μL PBS (sham animals). Animals were fed exclusively on a special rodent diet (Harlan Laboratories, Inc.; Tekland 2018S) to reduce autofluorescence.

In vivo and *ex vivo* fluorescence imaging

Mice bearing brain tumors derived from Gli36Δ5 or U87-MG cells were administered with compounds at 1 nmol/g via tail vein injection. *In vivo* competition assays were done with mixture of compound 2 and 10-fold concentration of nonlabeled probe 5. Before injection, mice were anesthetized with isoflurane and subjected to tomographic and spectral fluorescence imaging. One hour after injection, animals were re-imaged. Brains were then extracted and imaged. The excised brains were embedded in Tissue-Tek optimum cutting temperature for cryosections for immunohistochemistry (IHC). Fluorescence-mediated molecular tomography (FMT) images were obtained using FMT2500 (Perkin-Elmer), and 3-dimensional reconstructions of fluorescent signals were acquired using the accompanying software TrueQuant. Quantitative fluorescent signals for Cy5.5 of compound 2 were calibrated as per manufacturer's instructions using the 680-channel. Region of interest (ROI) assigned on the basis of the precise placement of cells during implantation at 3 to 4 mm into the brain. ROI was corroborated with fluorescent signals from *ex vivo* imaging. Fluorescent multispectral images were obtained using the Maestro *In-Vivo* Imaging System (CRi, Inc.). The yellow filter set appropriate for Cy5.5 was used for emission and excitation light. The tunable filter was automatically stepped in 10-nm increments whereas the camera captured images at a constant exposure of 200 ms. Fluorescence images were acquired before treatment, immediately after and 1.5 hours after treatment. To compare signal intensities, ROIs were selected over the tumor or nontumor areas, and the change in fluorescence signal over baseline was determined. The spectral fluorescent images consisting of autofluorescence spectra and imaging probe were captured and unmixed on the basis of their spectral patterns. The total signal in the ROI defined in photons measured at the surface of the animal was divided by the area (in pixels). Spectral libraries were generated by assigning spectral peaks to background and fluorescence probe on tissue. The spectral libraries were manually computed using the Maestro software, with each tissue used as its own background control.

IHC of cryosection of brain tissue

Sections (2 mm) of whole mouse brains implanted with Gli36Δ5 cells were fixed with 4% paraformaldehyde, cryosectioned onto microscope slides, rinsed with PBS, and blocked with 1% host serum for 30 minutes at room temperature. Sections were incubated with primary antibody at room temperature for 2 hours. Antibodies used were mouse anti-human wild-type EGFR (1:100 dilution; clone DAK-H1-WT, Dako cat. no. M7289). The coverslips were then rinsed with PBS and counterstained with DAPI for 10 minutes at room temperature to visualize the nuclei. After a final rinse with PBS, the slides were mounted with coverslips using Fluor-Mount aqueous media, sealed with nail polish, and observed using epifluorescence microscopy.

Western blotting

Cell extracts (50 μg) were fractionated using SDS-PAGE and transferred onto a nitrocellulose membrane. Immunoblotting was done using a 1:500 dilution of an antibody against wild-type EGFR (DAKO, DAK-H1-WT) or a 1:500 dilution of a specific antibody against mutant EGFRvIII (Bioss Inc., cat# bs-2558R). Horseradish peroxidase–conjugated secondary antibodies against mouse IgG (Chemicon) or rabbit IgG (Amersham) were used. Bands were detected using an enhanced chemiluminescence detection system (Pierce).

Statistical analysis

Analyses of data were achieved with GraphPad Prism version 4.00, GraphPad Software. Binding affinity was determined with nonlinear regression analysis with one site binding hyperbola with an equation: $Y = B_{max} \times X / (K_d + X)$, where B_{max} is the maximal binding site and the K_d is the concentration required to reach half-maximal binding. ANOVA analysis at 95% confidence interval (CI) was used to compare treatments (*, $P > 0.05$; **, $P > 0.01$; confidence interval, ***, $P > 0.001$). To compare live animal FMT, nonparametric one-way ANOVA analyses (Kruskal–Wallis tests) and the median differences were considered significant with $P = 0.0220$.

Results

The goal of these studies was to develop a peptide-based NIRF probe that would cross the BBTB and selectively bind to brain tumor cells overexpressing EGFR. For these studies, we used a peptide discovered through phage display screening against purified human EGFR (9). The peptide was modified to include linkers and a NIRF dye (Fig. 1). To determine the optimal space between the NIRF dye and the peptide, we designed and synthesized a series of peptides to include increasing numbers of discrete ethylene glycol units to serve as linkers between a Cy5.5 and the N-terminal end of the peptide. Cy5.5 and EGFpep were either directly linked or linked via 1, 2, or 3 units of discrete ethylene glycol (AEEA) moieties (Table 1). To determine which of the compounds optimally interacts with cells expressing EGFR, the apparent binding for each bioconjugate was fluorometrically determined from a saturation binding assay (16) *in vitro* using a human GBM cell line overexpressing EGFR and Gli36Δ5 (Table 1). Compounds 1, 2, 3, and 4 all bound to the cells with affinities in the micromolar range. Compound 2, which had one linker, had the highest apparent affinity with a K_d at least 2-fold better than compound 1, which had no ethylene linker, 8.9 to 18.5 μmol/L respectively. Compounds 3 and 4 have weaker affinities with K_d of 64.4 and 123.0 μmol/L, respectively.

Published OnlineFirst July 17, 2012; DOI: 10.1158/1535-7163.MCT-12-0211

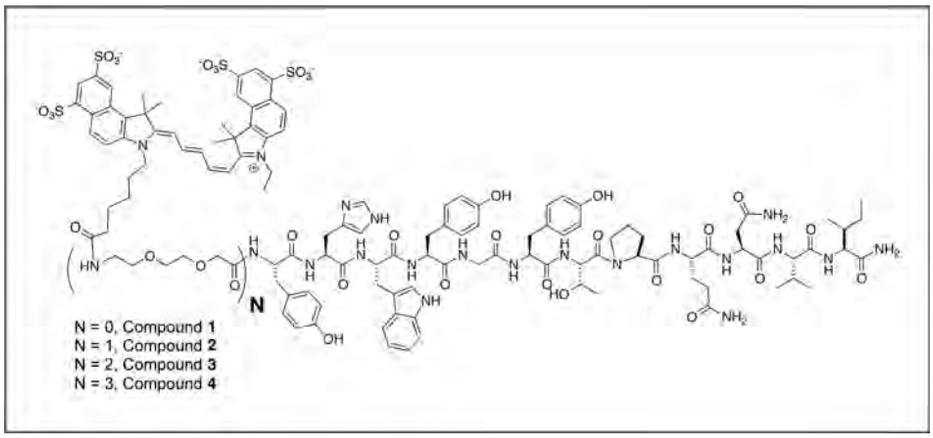

Figure 1. EGFR peptide ligands (EGF_{pep}) have been used in this study. EGF_{pep} is conjugated to a near-infrared fluorophore, Cy5.5, linked with up to 3 units of amino-ethoxy-ethoxy-acid (AEEA) at the N-terminal amine of the peptide.

We next used immunofluorescence microscopy to determine the fate of the peptide complexes once they bound to glioblastoma cells expressing EGFR. As predicted from the affinity measurements compound 2, which had the highest affinity, also showed the greatest accumulation of fluorescence after incubation with Gli36Δ5 cells (Fig. 2A). Neither compound 1 (no linker) nor either of the molecules with greater linker numbers (compounds 3 and 4) was taken up by the cells to the same extent as compound 2. Interestingly, the peptide with the longest linker and the worst binding affinity, compound 4, was taken up by cells better than compound 3 (Fig. 2B). When tested against U87-MG cells, which express much lower levels of the EGFR, no cellular uptake for any of the compounds was observed (Fig. 2C).

We next tested the ability of these compounds to target EGFR-expressing tumors implanted within the brains of mice. For these studies, mice were orthotopically implanted with Gli36Δ5 cells. Approximately 10 days after implantation, the animals were administered 1 nmol/g via tail vein injection and sacrificed 1 hour later. Brains were harvested and imaged *ex vivo* for accumulation of the imaging probe. As a control for specificity, we synthesized a Cy5.5-labeled scrambled peptide, compound 6, using the amino acid residues of the parent peptide (compound 5) in random order. Compound 2 targeted the tumor efficiently, accumulating 1.1% of injected dose (Fig. 3A, left graph). In contrast, compound 6 did not target the tumor with delivery of only 0.006% of the injected dose. To further assess specificity, animals that bore Gli36Δ5 brain tumors were administered compound 2 alone or in the presence of a 10-fold excess of unlabeled peptide (compound 5). In animals that received only compound 2, there was significant tumor-associated fluorescence. In contrast, when a 10-fold excess of competitor peptide was coadministered with compound 2, there was approximately a 60% decrease in accumulation of the probe, (Fig. 3A, right graph). Imaging and quantification of identical ROIs taken on the contralateral brain showed little uptake of the probe (data not shown).

To show that the uptake was associated with human EGFR expression on the Gli36Δ5 cells, the resected brains were fixed and subjected to IHC with monoclonal antibodies specific for human EGFR (Fig. 3B). These results have shown that only cells that expressed human EGFR were associated with Cy5.5 fluorescence. Notably, no Cy5.5 signal was associated with surrounding mouse brain.

Our final test for compound 2 was to determine whether it would be useful for noninvasive *in vivo* detection and discrimination of tumors differentially expressing EGFR. For these studies, mice were orthotopically implanted with either Gli36Δ5 cells, which express high EGFR, or

Table 1. The sequences of the peptides studied and the corresponding apparent binding affinities (K_d) from saturation binding assays

Compound	Peptide (EGF_{pep})	K_d, μmol/L
1	Cy5.5-YHWYGYTPQNVI-amide	18.5 ± 3.9
2	Cy5.5-$(AEEA)_1$-YHWYGYTPQNVI-amide	8.9 ± 3.7
3	Cy5.5-$(AEEA)_2$-YHWYGYTPQNVI-amide	64.4 ± 24.6
4	Cy5.5-$(AEEA)_3$-YHWYGYTPQNVI-amide	123.0 ± 174.0
5	YHWYGYTPQNVI-amide (GE11-amide)	ND
6	Cy5.5-$(AEEA)_1$-NYQTPVYGWIYH-amide (scrambled)	ND

Abbreviation: ND, not determined.

Published OnlineFirst July 17, 2012; DOI: 10.1158/1535-7163.MCT-12-0211

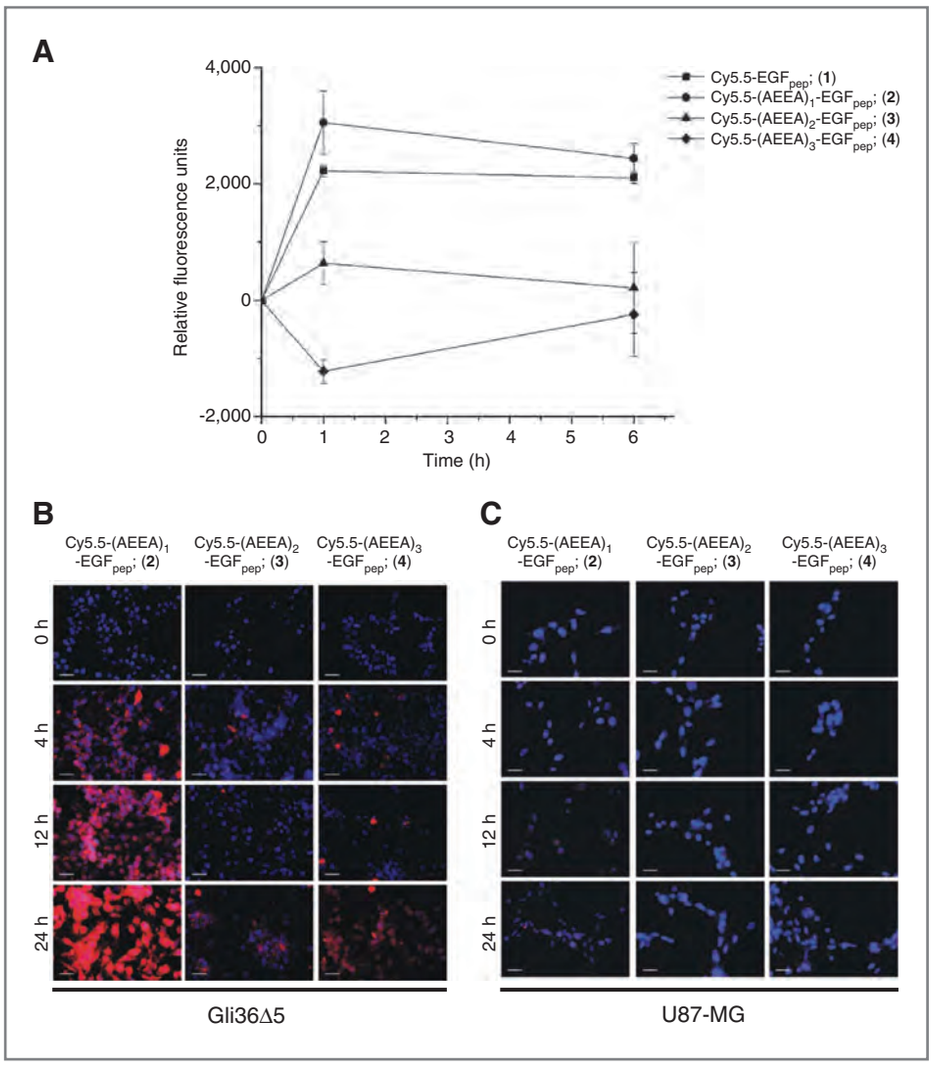

Figure 2. *In vitro* studies of the peptides with different linker lengths. A, Gli36Δ5 cells were incubated with 1 μmol/L of compounds 1 to 4 [Cy5.5-$(AEEA)_n$-EGF_{pep}], and the cell associated fluorescence was measured using spectrofluorometry at the indicated times. Gli36Δ5 (B) and U87-MG (C) cells were incubated with 1 μmol/L compounds for the indicated times. Uptake of the compounds was assessed using epifluorescence microscopy. Representative images are shown. Images were taken at ×40 magnification. Scale bar, 50 μm.

U87-MG cells, which express relatively low EGFR levels (Fig. 4A). Following implantation, the tumors were allowed to grow approximately 10 to 12 days and then mice were administered 1 nmol/g of compound 2 via tail vein injection. One hour after injection, the mice were anesthetized and the intensity of Cy5.5 fluorescence from the tumor was noninvasively quantified using FMT (Fig. 5A). The tumors formed from Gli36Δ5 cells had approximately 4-fold more fluorescence than either tumors formed with U87-MG cells or control sham surgeries (Fig. 5B). For Gli36Δ5 and U87-MG brain tumors, these fluorescence signals corresponded to injected doses of 1.1% and 0.27%, respectively. Statistical analyses showed that the median fluorescence signals between the 2 groups were significantly different (Fig. 5B). To corroborate these data, tumors were excised and subjected to *ex vivo* FMT and Maestro fluorescence imaging analyses (Fig. 5C and D). These measurements were in good agreement with those measurements made during the live animal imaging.

We also examined the expression of EGFRvIII in the cell lines. Western blots for the EGFRvIII on both U87-MG and Gli36Δ5 cells showed that the mutant receptor expression is similar for both cell lines (Fig. 4B). In addition, we examined A431 cells, a squamous carcinoma cell line, that expresses high levels of wild-type EGFR (Supplementary Fig. S1A and S1B). Saturation binding studies indicated that the K_d for binding was similar to that measured with Gli36Δ5 cells (Supplementary Fig. S1C). Furthermore, incubation of compound 2 with A431 cells displayed increasing fluorescence in the presence of the EGF ligand, which increases cycling of wild-type EGFR in cells (Supplementary Fig. S1D).

Discussion

The present study has identified a NIRF molecular imaging probe for cells overexpressing EGFR receptor that allows for noninvasive specific detection of tumors expressing the EGFR in live animals. The parent peptide sequenced used to derive compound 5 was initially

Published OnlineFirst July 17, 2012; DOI: 10.1158/1535-7163.MCT-12-0211

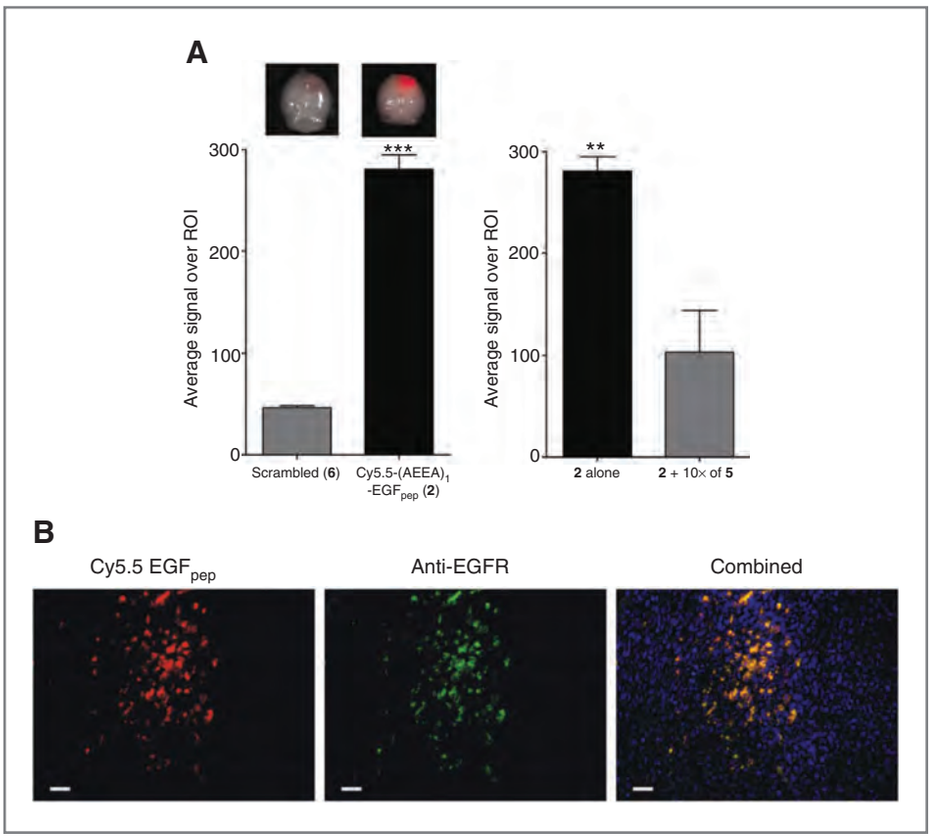

Figure 3. Near-infrared Cy5.5 labeled compound 2 is specific and selective to tumor cells overexpressing EGFR. A, specificity of the targeting was assessed using a scrambled peptide (6) and via competition against unlabeled parent peptide compound (5). Subjects bearing orthotopic brain tumors derived from Gli36Δ5 cells overexpressing EGFR were treated with (1 nmol/g mice) of compound 6 ($n = 3$) or compound 2 ($n = 5$). *Ex vivo* analysis of brain tissues showed that compound 2 targets the tumor significantly (***, $P > 0.0001$) more efficiently than the scrambled peptide 6. Representative images of the brain tumors are shown above the corresponding bars (left graph). When subjects bearing orthotopic brain tumors derived from Gli36Δ5 cells overexpressing EGFR were cotreated with compound 2 and a 10-fold excess of nonlabeled parent compound 5, the signal over the tumor region was significantly reduced. This suggests that the fluorescence labeling of tumor is specific to the peptide sequence of 2. B, the *ex vivo* brain fluorescence images were further validated with IHC of the brain tissues. The representative image shows the colocalization of EGFR-targeted probe (red) with cells expressing high levels of EGFR (green). Scale bar, 20 μm.

discovered by Li using phage display to identify peptides that bind to purified human EGFR (9). The parent peptide, GE11, has a binding affinity in the nanomolar range as determined from radioligand binding assays and also the additional advantage of being nonmitogenic—not inducing any proliferation of cells in *in vitro* assays (9). The initial applications of the GE11 peptide sequence used in compound **5** were for cancer diagnostics (17) and targeted drug delivery (18) but met with limited *in vivo* success.

Initially, Li used the GE11 peptide to deliver a gene–polymer complex to tumors (9). Song and colleagues then used the peptides conjugated to liposomes to deliver doxorubicin to tumors (18). However, the delivery of the liposomes was not much more effective than the untargeted controls and probably resulted primarily from enhanced permeability and retention (EPR) effects. Further studies by Master and colleagues used bioconjugation via the peptide N-terminal amine of the GE11 sequence to form co-block polymers with high molecular PEG to deliver photodynamic therapy agents to cells (19). Similarly, these studies did not greatly increase the targeting of PDT agents. For systemic administration of short peptides, it is known that C-terminal amides significantly increase the half-life stability *in vivo* (4). We surmised that conjugation of the GE11 peptide via its amine resulted in lower serum stability as well as poor *in vivo* targeting and drug delivery due in part to the free carboxylate at the C-terminus. We aimed to develop compound 5 into a fluorescence imaging probe for noninvasive detection of tumors overexpressing EGFR and, therefore, incorporated lessons from prior studies into our probe design by conjugating the peptide via its free carboxyl-terminal end.

A concern was that upon conjugation of the dye, the increased hydrophobicity and bulk of the bioconjugate might significantly perturb the interaction between the ligand and receptor. Thus, we decided to introduce spacers composed of discrete units of ethylene glycol between the peptide and the Cy5.5 dye. Direct conjugation of Cy5.5 to the parent peptide 5 resulted in a significant drop in binding affinity from a nanomolar to micromolar

Published OnlineFirst July 17, 2012; DOI: 10.1158/1535-7163.MCT-12-0211

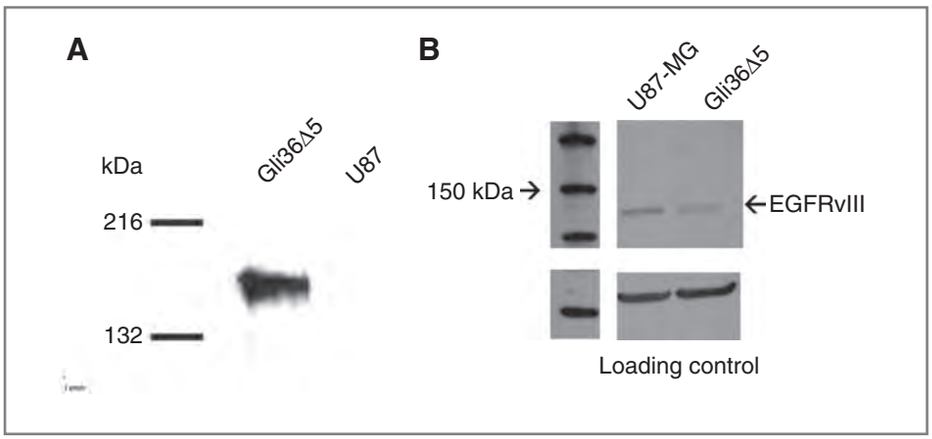

Figure 4. Differential expression levels of EGFR and EGFRvIII in Gli36Δ5 and U87-MG. A, Western blot analysis showing the relative levels of wild-type EGFR expressed in Gli36Δ5 and U87-MG glioblastoma cell lysates using an antibody specific to wild-type EGFR (DAKO, cat# M7289). B, Western blot analysis comparing the mutant EGFRvIII content in Gli36Δ5 and U87-MG tumor cells lines using an EGFRvIII-specific antibody (Bioss Inc., cat# bs-2558R). β-Actin was used a loading control. Densitometry analysis of Western blotting by ImageJ comparing the levels of EGFRvIII in Gli36Δ5 and U87-MG cells show similar content of 1,800 and 2,400 arbitrary units, respectively.

range. This degree of change in binding affinity is not uncommon in the modifications of individual parent peptides, particularly from peptides discovered the rough phage analysis (7, 9). The affinity was improved 2-fold to by inclusion of a single PEG spacer between the peptide and the Cy5.5 but still remained in the low micromolar range. Increased linker lengths did decrease affinity for the cellular EGFR, which may be due to additional bulk introduced by the linkers or to the linkers' interference with the binding site in the EGFR. Nevertheless, Cy5.5-labeled peptide compounds 1, 2, and, to a lesser extent, 4 were efficiently internalized into cells within hours. Despite the significant drop in affinity, the whole set of Cy5.5 compounds with different linker lengths provide a large range of affinities that could play an important role in different *in vivo* applications of the probes when better pharmacokinetics are needed and high affinities are not necessarily required for effective targeting to biomarkers.

The competition assays against nonlabeled compound 5 and comparisons with a scrambled sequence 6 suggest specificity for the binding of compound 2 to tumors overexpressing EGFR. To further assess this apparent specificity, we also tested the ability of compound 2 to bind to a brain tumor cell line that does not overexpress EGFR. In *in vitro* assays, we observed that compounds 2, 3, and 4 were not appreciably taken up by U87-MG cells (Fig. 2C), in which we showed that EGFR content was significantly lower than in Gli36Δ5 (Fig. 4A). The low level expression of EGFR in U87-MG is consistent with previous reports (3).

The parent peptide sequence used to derive compound 5 has been used as targeting sequence but has not been fully used for *in vivo* imaging of tumors in live animals, particularly human GBM orthotopic brain tumor models in mice. The *in vitro* results measuring differences in EGFR expression encouraged us to determine whether compound 2 could be used to noninvasively differentially detect tumors formed from cells expressing different levels of EGFR expression. Thus, in an orthotopic brain tumor model in live animals, we explored the use of compound 2 to differentially detect glioblastoma brain tumors derived from cell lines with high and low expression of EGFR. The live animal imaging was achieved with FMT, which provides good resolution and quantitative tomographic images of tumors (20). Analyses of the fluorescent tomographic images showed that tumor accumulation of compound 2 reflects the EGFR content of the tumors with Gli36Δ5 tumors accumulating significantly more fluorescence signal than U87-MG tumors. Along with the corresponding control conditions, which did not generate significant fluorescence, this suggests that compound 2 targets cells overexpressing EGFR. This uptake is significantly more than that measured with the scrambled control or for U87-MG cells treated with compound 2. The modest uptake measured in these latter cases is likely a result of the leaky tumor vasculature and EPR effects (21).

Cancer cells including gliomas have heterogeneous expressions of EGFR receptors and its mutant EGFRvIII. To show whether EGFR or its mutant form is responsible for the uptake we are measuring, we used Western blotting to measure the amount of EGFRvIII present in both U87-MG and Gli36Δ5 cells. These data (Fig. 4B) have shown that the level of EGFRvIII expressed in both cell types is approximately equal. In contrast, the wild-type EGFR is highly expressed in the Gli36Δ5 cells relative to the U87-MG (Fig. 4A). The uptake of compound 2 is markedly higher in Gli36Δ5 cells than in U87-MG cells for both *in vitro* (Fig. 2A and B) and *in vivo* studies (Fig. 5), suggesting that this receptor is responsible for the uptake that we measure.

We also measured the uptake of compound 2 in A431 cells, a cell line that expresses high levels of the wild-type

Published OnlineFirst July 17, 2012; DOI: 10.1158/1535-7163.MCT-12-0211

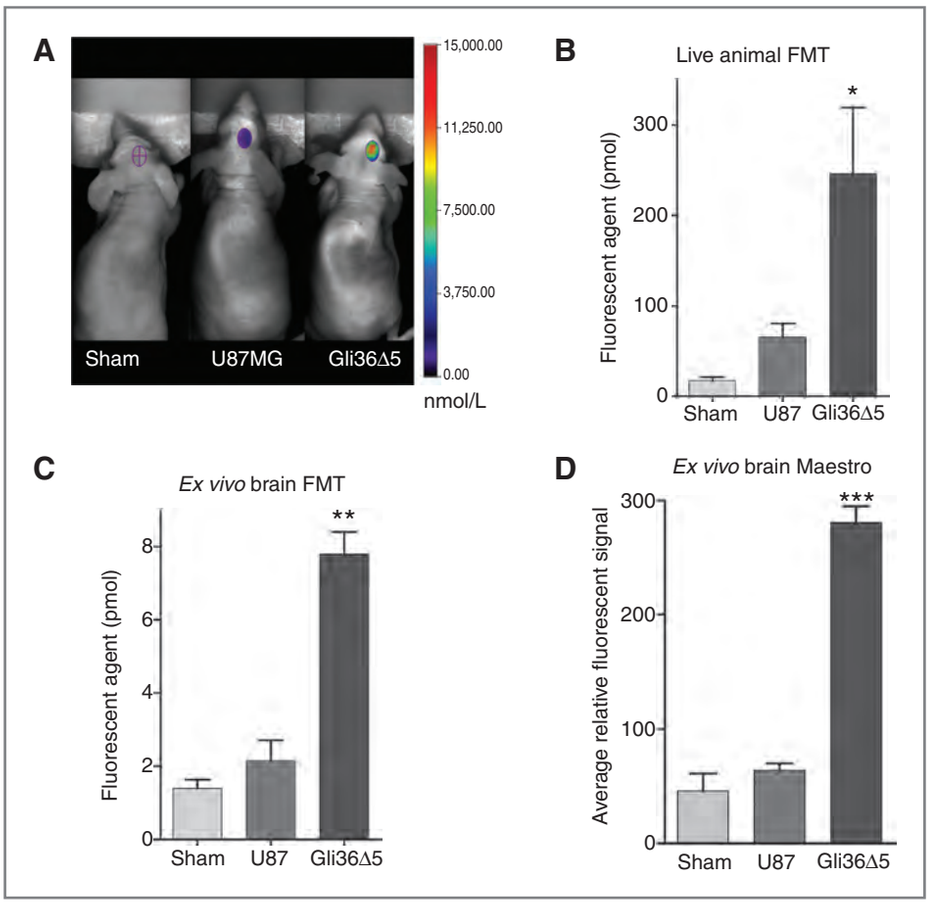

Figure 5. Application of near-infrared EGFR probe for *in vivo* differential detection of tumors expressing different EGFR levels. A, representative image of FMT 3-dimensional reconstruction showing the targeting of compound **2** to brain Gli36Δ5 orthotopic brain tumors. Sham, U87-MG, and Gli36Δ5 shows 272, 1,608, and 9,271 nmol/L amounts of fluorescence in the matching ROIs. B, targeting of brain tumor in live animals using FMT was quantified and the graph shows higher detection of tumor with mice bearing the Gli36Δ5 tumor (*, $P > 0.05$). C, live animal FMT imaging of tumors was further assessed by FMT imaging of explanted brains. With similar trends observed in live animal study, analyses of the reconstructed images of *ex vivo* brain tissues showed a significant differential detection between mice bearing Gli36Δ5 (high EGFR) brain tumor and mice bearing U87-MG (low EGFR) cells. Compound 2 targeting detects differential levels of EGFR between glioblastoma types. Sham ($n = 2$); U87-MG ($n = 3$); Gli36Δ5 ($n = 5$); ANOVA (**, $P > 0.01$). D, *ex vivo* brain samples were also examined using Maestro. The Maestro image analysis reflects the FMT analyses where fluorescence signal is significantly more in mice bearing Gli36Δ5 than in U87-MG glioblastoma cell types, ANOVA (***, $P > 0.001$).

EGFR. These studies indicated a similar K_d of binding for compound 2 to the cells, and when stimulated with EGF, the cells increased the level of uptake of compound 2. Taken together with our *in vitro* and *in vivo* uptake studies, these data suggest that the wild-type EGFR is the receptor responsible for the uptake of compound 2. These results are consistent with reports that GE11-based molecules bind to the wild-type EGFR in various cell lines including A431 (9, 19).

In the brain tumor animal models, compound 2 generated significant fluorescent signals associated with the tumor relative to normal tissues. However, the brain tumor model used in these studies results in a leaky vasculature when assessed by iron oxide nanoparticle imaging (22) and probably explains the ability of this probe to selectively light-up EGFR-expressing tumors in the brain. There are, however, reports that some peptides cross the intact blood–brain barrier (BBB), more so for peptides based on phage display sequences. The extent to which these peptides may cross intact BBB still needs to be investigated (8).

EGFR is an attractive drug target for various cancers because the cell surface tyrosine kinase is often associated with its overexpression, which might have a role in the progression of the tumor. Imaging of differential expression of EGFR in various cancers including colorectal and head and neck squamous carcinoma, and non–small cell lung cancer has been explored extensively with positron emission tomography (PET) or PET/computed tomographic (CT) imaging modalities radiolabeled EGF ligand (23) and EGFR-targeted antibodies (24, 25), peptides (17), and small molecules (26). The ability to noninvasively observe EGFR levels of tumors in subjects is increasingly important for the purpose of diagnosis of cancer and longitudinal monitoring of drug therapies. Aberrant overexpression of EGFR is also

Published OnlineFirst July 17, 2012; DOI: 10.1158/1535-7163.MCT-12-0211

found in 40% to 50% of high-grade gliomas and is ultimately correlated with poor prognosis and drug resistance (1, 2).

There is a significant need to identify tumor margins especially in settings where tissue-sparring resections of tumors is required, such as in brain tumor removal (27–30). Recently, clinical trials in Europe have begun to use fluorescence-guided surgical techniques to achieve more complete brain tumor resections (27–31). Indeed, most recently, intra-operative microscopic techniques in combination with molecular imaging probes specific for tumor markers, such as folic acid receptors and transpeptidases, have shown a significant role in future surgical and therapeutic approaches for targeted fluorescence imaging probes (32, 33). Here, we have developed a fluorescent probe that images tumors overexpressing EGFR and can potentially be used to understand the expression of EGFR in the research setting but also has potential applicability to human disease, including receptor detection during surgical interventions.

Conclusions

We have developed a NIRF probe targeting the EGFR, based on a phage display peptide against the receptor. Various linker lengths between the fluorescence probe and the peptide generated various binding affinities. The lead compound 2 was used to noninvasively detect tumors that expressed different levels of EGFR in live animal imaging models, which was validated using various methods. Thus, we have shown targeting to tumors overexpressing EGFR. We are currently exploring the probe's selectivity among the EGFR mutants. The probe could prove invaluable for cancer research as a diagnostic tool for longitudinal studies and could translate into use as a guide for tumor resections in patients in the future.

Disclosure of Potential Conflicts of Interest

J.P. Basilion is a Board of Trustees member and a co-founder of Akrotome Imaging Inc. He has received other commercial research support, has ownership interest (including patents), and is a consultant/advisory board member of Akrotome Imaging Inc. No potential conflicts of interest were disclosed by the other authors.

Authors' Contributions

Conception and design: R.S. Agnes, A.-M. Broome, J.P. Basilion
Development of methodology: R.S. Agnes, A.-M. Broome, J. Wang, J.P. Basilion
Acquisition of data (provided animals, acquired and managed patients, provided facilities, etc.): R.S. Agnes, A.-M. Broome, J. Wang, K. Lavik
Analysis and interpretation of data (e.g., statistical analysis, biostatistics, computational analysis): R.S. Agnes, A.-M. Broome, J.P. Basilion
Writing, review, and/or revision of the manuscript: R.S. Agnes, A.-M. Broome, J.P. Basilion
Administrative, technical, or material support (i.e., reporting or organizing data, constructing databases): R.S. Agnes, J. Wang,
Study supervision: A.-M. Broome, J.P. Basilion

Acknowledgments

The authors thank Lebing Wang for technical assistance.

Grant Support

The study was supported by National Foundation for Cancer Research (NFCR; J.P. Basilion); State of Ohio Biomedical Research Commercialization (ODD Tech 09-004; J.P. Basilion); National Institutes of Health (NIH-R01CA109620 to J.P. Basilion; NIH-U24CA110943 to J.L. Duerk; and NIH-R01EB12099 to A.-M. Broome).

The costs of publication of this article were defrayed in part by the payment of page charges. This article must therefore be hereby marked *advertisement* in accordance with 18 U.S.C. Section 1734 solely to indicate this fact.

Received February 27, 2012; revised June 29, 2012; accepted July 6, 2012; published OnlineFirst July 17, 2012.

References

1. Libermann TA, Nusbaum HR, Razon N, Kris R, Lax I, Soreq H, et al. Amplification, enhanced expression and possible rearrangement of EGF receptor gene in primary human brain tumours of glial origin. Nature 1985;313:144–7.
2. Schlegel J, Merdes A, Stumm G, Albert FK, Forsting M, Hynes N, et al. Amplification of the epidermal-growth-factor-receptor gene correlates with different growth behaviour in human glioblastoma. Int J Cancer 1994;56:72–7.
3. Nagane M, Levitzki A, Gazit A. Drug resistance of human glioblastoma cells conferred by a tumor-specific mutant epidermal growth factor receptor through modulation of Bcl-XL and caspase-3-like proteases. Proc Natl Acad Sci U S A 1998;95:5724–29.
4. Hruby VJ, Agnes RS, Cai C. Design of peptide agonists. Methods Enzymol 2002;343:73–91.
5. Smith GP. Filamentous fusion phage: novel expression vectors that display cloned antigens on the virion surface. Science 1985;228:1315–17.
6. Pasqualini R, Ruoslahti E. Organ targeting *in vivo* using phage display peptide libraries. Nature 1996;380:364–66.
7. Hao J, Serohijos AWR, Newton G, Tassone G, Wang Z, Sgroi DC, et al. Identification and rational redesign of peptide ligands to CRIP1, a novel biomarker for cancers. PLoS Comput Bio 2008;4:e1000138.
8. Staquicini FI, Ozawa MG, Moya CA, Driessen WHP, Barbu EM, Nishimori H, et al. Systemic combinatorial peptide selection yields a non-canonical iron-mimicry mechanism for targeting tumors in a mouse model of human glioblastoma. J Clin Invest 2011;121:161–73.
9. Li Z. Identification and characterization of a novel peptide ligand of epidermal growth factor receptor for targeted delivery of therapeutics. FASEB J 2005;19:1978–85.
10. Weissleder R. Molecular imaging in cancer. Science 2006;312:1168–71.
11. Weissleder R. Imaging in the era of molecular oncology. Nature 2008;452:580–9.
12. Rudin M, Weissleder R. Molecular imaging in drug discovery and development. Nat Rev Drug Disc 2003;2:123–31.
13. Agnes RS, Lee Y-S, Davis P, Ma S-w, Badghisi H, Porreca F, et al. Structure-activity relationships of bifunctional peptides based on overlapping pharmacophores at opioid and cholecystokinin receptors. J Med Chem 2006;49:2868–75.
14. Gruber HJ, Hahn CD, Kada G, Riener CK, Harms GS, Ahrer W, et al. HYPERLINK "http://www.ncbi.nlm.nih.gov/pubmed/10995214" Anomalous fluorescence enhancement of Cy3 and cy3.5 versus anomalous fluorescence loss of Cy5 and Cy7 upon covalent linking to IgG and noncovalent binding to avidin. Bioconjug Chem. 2000; 11; 696-704.
15. Tyminski E. Brain tumor oncolysis with replication-conditional herpes simplex virus type 1 expressing the prodrug-activating genes, CYP2B1 and secreted human intestinal carboxylesterase, in combination with cyclophosphamide and irinotecan. Cancer Res 2005;65:6850–7.
16. Handl HL, Vagner J, Yamamura HI, Hruby VJ, Gillies RJ. Development of a lanthanide-based assay for detection of receptor-ligand interactions at the delta-opioid receptor. Anal Biochem 2005;343:299–307.

Published OnlineFirst July 17, 2012; DOI: 10.1158/1535-7163.MCT-12-0211

17. Dejesus OT. Synthesis of [(64)Cu]Cu-NOTA-Bn-GE11 for PET imaging of EGFR-rich tumors. Curr Radiopharm 2012;5:15–8.
18. Song S, Liu D, Peng J, Sun Y, Li Z, Gu J-R, et al. Peptide ligand-mediated liposome distribution and targeting to EGFR expressing tumor *in vivo*. Int J Pharm 2008;363:155–61.
19. Master AM, Qi Y, Oleinick NL, Gupta AS. EGFR-mediated intracellular delivery of Pc 4 nanoformulation for targeted photodynamic therapy of cancer: *in vitro* studies. Nanomedicine 2012;8:655–64.
20. Ntziachristos V. Fluorescence molecular imaging. Ann Rev Biochem Eng 2006;8:1–33.
21. Fang J, Nakamura H, Maeda H. The EPR effect: unique features of tumor blood vessels for drug delivery, factors involved, and limitations and augmentation of the effect. Adv Drug Delivery Rev 2011;63:136–51.
22. Pardridge WM. Drug and gene targeting to the brain with molecular Trojan horses. Nat Rev Drug Disc 2002;1:131–9.
23. Li W, Niu G, Lang L, Guo N, Ma Y, Kiesewetter DO, et al. PET imaging of EGF receptors using [(18)F]FBEM-EGF in a head and neck squamous cell carcinoma model. Eur J Nucl Med Mol Imaging 2012;39:300–8.
24. Achmad A, Hanaoka H, Yoshioka H, Yamamoto S, Tominaga H, Araki T, et al. Predicting cetuximab accumulation in KRAS wild-type and KRAS mutant colorectal cancer using (64) Cu-labeled cetuximab positron emission tomography. Cancer Sci 2012;103:600–5.
25. Terwisscha van Scheltinga AG, van Dam GM, Nagengast WB, Ntziachristos V, Hollema H, Herek JL, et al. Intraoperative near-infrared fluorescence tumor imaging with vascular endothelial growth factor and human epidermal growth factor receptor 2 targeting antibodies. J Nucl Med 2011;52:1778–85.
26. Memon AA, Weber B, Winterdahl M, Jakobsen S, Meldgaard P, Madsen HHT, et al. PET imaging of patients with non-small cell lung cancer employing an EGF receptor targeting drug as tracer. Br J Cancer 2011;105:1850–5.
27. Claus EB, Horlacher A, Hsu L, Schwartz RB, Dello-Iacono D, Talos F, et al. Survival rates in patients with low-grade glioma after intraoperative magnetic resonance image guidance. Cancer 2005;103:1227–33.
28. Keles GE, Anderson B, Berger MS. The effect of extent of resection on time to tumor progression and survival in patients with glioblastoma multiforme of the cerebral hemisphere. Surg Neurol 1999;52:371–9.
29. McPherson CM, Sawaya R. Technologic advances in surgery for brain tumors: tools of the trade in the modern neurosurgical operating room. J Nat Compr Canc Netw 2005;3:705–10.
30. Stummer W, Reulen H-J, Meinel T, Pichlmeier U, Schumacher W, Tonn J-C, et al. Extent of resection and survival in glioblastoma multiforme: identification of and adjustment for bias. Neurosurg 2008;62:564–76.
31. Laws ER, Parney IF, Huang W, Anderson F, Morris AM, Asher A, et al. Survival following surgery and prognostic factors for recently diagnosed malignant glioma: data from the Glioma Outcomes Project. J Neurosurg 2003;99:467–73.
32. Yoo H, Kim JW, Shishkov M, Namati E, Morse T, Shubochkin R, et al. Intra-arterial catheter for simultaneous microstructural and molecular imaging *in vivo*. Nat Med 2011;17:1680–4.
33. Urano Y, Sakabe M, Kosaka N, Ogawa M, Mitsunaga M, Asanuma D, et al. Rapid cancer detection by topically spraying a gamma-glutamyltranspeptidase-activated fluorescent probe. Science Trans Med 2011;3:110ra9.

APPENDIX B

Bioconjugate Chemistry

Article

pubs.acs.org/bc

Optical Imaging of Targeted β-Galactosidase in Brain Tumors to Detect EGFR Levels

Ann-Marie Broome,*[,†,‡,§] Gopal Ramamurthy,[†] Kari Lavik,[†] Alexander Liggett,[†] Ian Kinstlinger,[†] and James Basilion[∥,⊥,#]

[†]Department of Radiology and Radiological Sciences, [‡]Center of Biomedical Imaging, and [§]Department of Neurosciences, Medical University of South Carolina, Charleston, South Carolina 29425, United States

[∥]Department of Biomedical Engineering, [⊥]Case Center for Imaging Research, and [#]The NFCR Center for Molecular Imaging, Case Western Reserve University, Cleveland, Ohio 44106, United States

ABSTRACT: A current limitation in molecular imaging is that it often requires genetic manipulation of cancer cells for noninvasive imaging. Other methods to detect tumor cells in vivo using exogenously delivered and functionally active reporters, such as β-gal, are required. We report the development of a platform system for linking β-gal to any number of different ligands or antibodies for in vivo targeting to tissue or cells, without the requirement for genetic engineering of the target cells prior to imaging. Our studies demonstrate significant uptake in vitro and in vivo of an EGFR-targeted β-gal complex. We were then able to image orthotopic brain tumor accumulation and localization of the targeted enzyme when a fluorophore was added to the complex, as well as validate the internalization of the intravenously administered β-gal reporter complex ex vivo. After fluorescence imaging localized the β-gal complexes to the brain tumor, we topically applied a bioluminescent β-gal substrate to serial sections of the brain to evaluate the delivery and integrity of the enzyme. Finally, robust bioluminescence of the EGFR-targeted β-gal complex was captured within the tumor during noninvasive in vivo imaging.

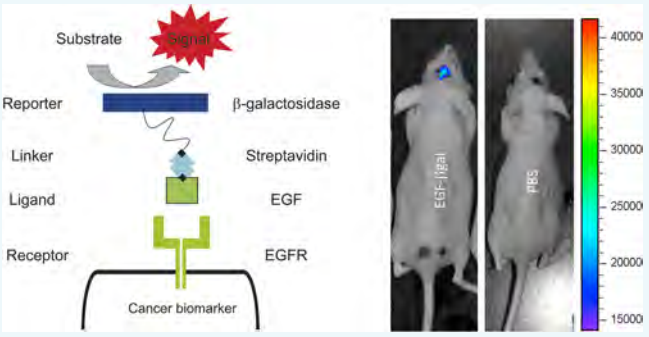

INTRODUCTION

β-Galactosidase (β-gal) is an enzyme that has been used heavily as a marker to detect gene expression, and several substrates exist to assay its presence in cells and tissue, including fixed tissue.[1,2] More recently investigators have sought to exploit the robust activity of β-gal enzyme for noninvasive imaging in biological systems that are genetically engineered to express β-gal.[3−5] Weissleder and co-workers have reported the use of DDAGO as an in vivo substrate for β-gal activity that fluoresces in the near-infrared (NIR) making it ideal for detection of β-gal activity expressed by genetically engineered 9L glioma cells. Although the excitation and emission spectra of this agent overlap significantly, these investigators were able to demonstrate measurable fluorescence dependent on β-gal expression from engineered 9L glioma cells or cancer cells infected in vivo with a virus driving expression of β-gal. Blau and co-workers have taken a different approach to imaging β-gal activity noninvasively in vivo.[4] In these studies, they utilized sequential reporter-enzyme luminescence to detect β-gal activity using Lugal substrate. Lugal is a caged luciferase substrate that requires "uncaging" by β-gal to become a substrate for luciferase. Using this agent the investigators were able to detect luminescence in vivo only from cells that expressed both luciferase and β-gal enzymes. Further, they demonstrated that systemic administration of β-gal conjugated antibodies could be used to selectively label cells in vivo and after Lugal injection generate luminescence signal identifying the location of the cells using noninvasive bioluminescence imaging, as long as the targeted cells had been engineered to express luciferase.

Another approach for the development of activated MRI contrast agents is receptor-induced magnetization enhancement, or RIME.[6,7] This contrast agent consists of two parts, a gadolinium complex and a β-glucuronidase substrate (β-D-glucopyranuronic acid). Consequently, β-glucuronidase activity endogenously expressed within tumor tissues could be evaluated. A more recent example of this is by Hanaoka et al. in which β-gal is exploited to remove a galactopyranose-masking group allowing a strong interaction to occur between the gadolinium complex and albumin.[8] The result is a slower molecular tumbling rate, leading to a stronger relaxivity. Based on findings of different relaxivity gaps for MR contrast agents, several groups have developed probes to report on different microenvironment or enzyme expressions, including hypoxic conditions as well as peroxidase and esterase activity.[9−14]

Relevant to the techniques described within this work, Meade and co-workers also developed a modified sugar substrate

Received: December 17, 2014
Revised: March 14, 2015
Published: March 16, 2015

DOI: 10.1021/bc500597y
Bioconjugate Chem. 2015, 26, 660−668

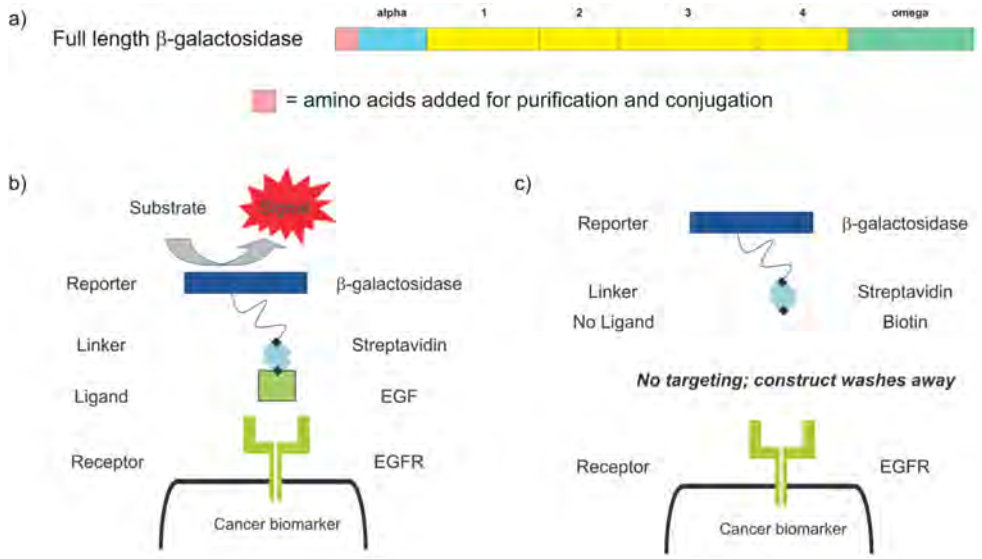

Figure 1. Engineering a reporter complex to identify cancer biomarkers exogenously. (a) Modified domains of full-length β-gal. (b) Targeted reporter activity. (c) Lack of reporter activity without targeting.

containing a gadolinium chelate (EGadMe) to enhance the imaging contrast of β-gal in magnetic resonance imaging (MRI). In the absence of β-gal, EGadMe exhibits a water inaccessible conformation; in the presence of β-gal, the enzyme cleaves the sugar (galactopyranose) from EGadMe causing an increase in T_1 relaxivity.[15] MRI was conducted in living *X. laevis* embryos transfected with plasmid DNA of the β-gal gene (*lacZ*) and showed significant signal intensity enhancement. However, there are limitations on requiring genetic manipulation of cancer cells for noninvasive imaging, and other methods to detect tumor cells in vivo using β-gal will be required. Here, we report the development of a platform system for linking β-gal to any number of different ligands or antibodies for in vivo targeting to tissue or cells, without the requirement for genetic engineering of the target cells prior to imaging.

For our studies β-gal has been engineered to contain a His tag for purification and a biotinylation signal.[16] Once expressed in bacteria, these proteins can be easily purified over a nickel column and then complexed via streptavidin (SA) to any ligands or antibodies to target the enzyme to biomarkers in vivo.[16] Administration of different fluorescent or bioluminescent substrates for β-gal can then be used to detect the location of the enzyme (Figure 1). In addition, we utilize a fluorescent marker conjugated on the SA to provide an additional means of gaining histological and cellular positional information.

We were interested in determining whether β-gal could be used to assess the expression of endogenous biomarkers in brain tumors that have been reported to be involved with malignant transformation and cancer growth. The most common gain of function mutation observed in invasive phenotypes associated with high-grade gliomas of the classical subtype, occurring in 30–50% of all glioblastomas, is the amplification and overexpression of the epidermal growth factor receptor (EGFR).[17−21] Tumors that overexpress EGFR have increased activity associated with uncontrolled cell growth accompanied by decreased apoptosis and increased angiogenesis and also activate other genes that promote cancer growth through such means as invasion and metastasis, as well as resistance to chemotherapy and radiotherapy.[22−24] Because of its relatively small size, we therefore utilized an epidermal growth factor (EGF) engineered peptide to target EGFR on the surface of brain tumor cells and demonstrate noninvasive imaging of EFGR expression.[25] Further, we are able to demonstrate that these complexes are able to detect differences in expression of EGFR between different brain tumors in vivo. The development of such a reporter provides the opportunity to, in the future, image multiple receptors by targeting the reporter enzyme to the surface receptor and then targeting an imageable substrate to a different cell surface receptor, thereby requiring the expression of two biomarkers to drive signal generation.

RESULTS

β-Galactosidase (β-gal) is a classic reporter enzyme used to examine the expression of various proteins in vitro and in vivo. The enzyme functions as a tetramer composed of 4 individual monomers with 5 domains. It is very robust such that its activity can be assayed even after fixation of cells. We wondered whether this robust reporter enzyme could be used to measure the level of cell surface receptors present on brain tumors in an orthotopic mouse model of human brain tumors. Using molecular engineering techniques, full-length β-gal was engineered to have two tags: (1) His-tag for protein purification over an affinity column and (2) biotin-tag for complexing the β-gal to SA to form an imaging complex that can be delivered exogenously (Figure 1a).[16] We have used this construct to produce a platform-based approach for a molecular imaging strategy able to noninvasively measure the level of cell surface receptors expressed on tumors in vivo. As previously demonstrated, the constructs in Figure 1b can be synthesized, purified, and retain β-gal activity.[16] A control construct was also created which did not contain a targeting moiety and thus subject to clearance from the local environment (Figure 1c).

We first sought to demonstrate targeting of this construct outlined in Figure 1 to cells that express EGFR. The genetically modified β-gal was purified and concentrated prior to use. After confirmation of SA binding to β-gal, the complete EGF-β-gal complex was prepared by combining biotinylated EGF peptide and biotinylated-β-gal and mixing them in the presence of Alexa 647-conjugated SA at molar ratios of 1:3:1. Constructs were then added to Gli36Δ5 cells, which overexpress EGFR in vitro, and

DOI: 10.1021/bc500597y
Bioconjugate Chem. 2015, 26, 660−668

binding and uptake of the EGF-β-gal complex was monitored by fluorescence microscopy using the fluorophore-labeled SA contained within the complex (Figure 2a). The construct

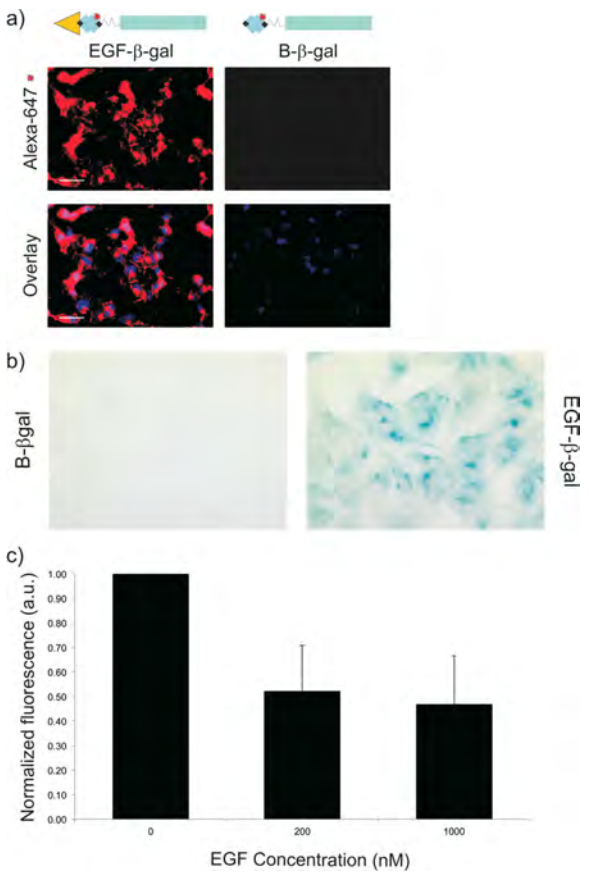

Figure 2. In vitro activity of targeted-β-galactosidase. (a) Gli36Δ5 cells incubated with either EGF-β-gal or B-β-gal were monitored by fluorescence microscopy using the fluorophore-labeled SA (647 nm) contained within the complex. (b) Internalized β-gal activity as shown by staining with the β-gal substrate, 5-bromo-4-chloro-3-indolyl-β-D-galactopyranoside (X-gal). (c) Internalization of EGF-β-gal was inhibited by full length EGF.

seemed to concentrate in discrete vesicles surrounding the perinuclear region of the cell as observed in Figure 2a and b. Once internalized into the cell, the β-gal retained enzyme activity as shown by staining with the β-gal substrate, 5-bromo-4-chloro-3-indolyl-β-D-galacto-pyranoside (X-gal) (Figure 2b). Internalization of the EGFR-targeted β-gal complexes was competitively inhibited by full-length EGF (50% inhibition) within a 4 h incubation period (Figure 2c).

We next tested the utility of the construct to accumulate in tumors expressing EGFR using an orthotopic mouse model for brain tumors. Glioma cells, Gli36Δ5, were stereotactically implanted in the brains of mice and grown for approximately 10 days as per IUCAC approved protocols. Mice were intravenously injected with 1 mg kg^{-1} body weight of either EGF-β-gal (targeted) or B-β-gal (nontargeted), both of which incorporated Alexa 647-labeled SA to easily visualize targeted-complex uptake following tissue preparation (Figure 3a). Targeted-β-gal crossed the blood-brain-tumor-barrier (BBTB) as measured by fluorescence molecular tomography in living mice (Figure 3b). Approximately 3−5% (~133 nM) of the injected dose accumulated within the tumor within 4 h. After 4 h, the mice were euthanized and the brains were removed and imaged whole and then serially transected into 2 mm sections and imaged again ex vivo using a Maestro fluorescence imaging system (Figure 3c, top panels). EGF-β-gal specifically accumulates in the tumor within 4 h. In contrast, nontargeted B-β-gal did not accumulate in the tumor as indicated by a lack of fluorescent signal, but presumably remained in the ventral cerebral and cerebellar arteries of the brain (Figure 3c, bottom panels).

Serial sections of the brains were cryosectioned and counterstained with DAPI to delineate cell nuclei. Fluorescence images captured at 100× magnification clearly showed significant EGF-β-gal uptake within the tumor and internalization within the cells' cytoplasm. Cryosections of brain containing the tumor region were then counterstained with anti-EGFR (Figure 3d) or anti-vimentin (Figure 3e) and visualized using epifluorescence microscopy. These studies indicated that EGFR is heterogeneously expressed within the tumor (green) and that targeted-β-gal complex (red) accumulates specifically in glioma cells overexpressing EGFR (Figure 3d). Vimentin staining, a standard pro-invasive intermediate filament tumor marker, identified implanted cells within the orthotopic mouse model which were of human origin, i.e., Gli36Δ5 cells, and demonstrated that targeted-β-gal complex (red) only colocalized within human cells expressing vimentin (green) (Figure 3e). Little to no β-gal complex was found within other regions of the brain (data not shown).

We then determined whether β-gal activity was maintained by the targeted complex. For these studies, orthotopic brain tumors implanted as described above were used. After approximately 10 days of growth, tumors were harvested by removing the intact mouse brain and then sectioning it into 2 mm sections. Following sectioning, a bioluminescent β-gal substrate, Galacto-Light Plus,[26] was topically applied to the ex vivo brain serial sections to evaluate the delivery and integrity of enzyme across the BBTB (Figure 4a). Further, the targeting ability and enzymatic activity in Gli36Δ5-derived brain tumors, expressing high levels of EGFR, was compared to brain tumors implanted with U87 cells expressing low levels of EGFR. Robust bioluminescence was captured within the tumor overexpressing EGFR after 3 min, indicating that β-gal maintained its activity. Minimal β-gal activity was observed in U87-derived tumors, which express very low levels of the EGFR protein as previously determined by Western blot.[27] The luminescence was quantified and Gli36Δ5 tumors possessed 3−4-fold more enzymatic activity than U87 tumors (Figure 4b). Qualitatively this correlated well with the increase in average fluorescence intensity recorded between Gli36Δ5 tumors and U87 tumors. Tumor cryosections counterstained with EGFR antibody (green) and DAPI (blue) demonstrated the differences in both the level of EGFR expression and EGFR-targeted uptake of the β-gal complex within the two tumor types, high EGFR expression and low EGFR expression, respectively (Figure 4c). Western blot analysis confirmed the higher expression levels of EGFR observed in Gli36Δ5 cells versus U87 cells.[27]

The next step in these studies was to demonstrate that complex formation could be imaged noninvasively in living mice. Mice containing orthotopically implanted Gli36Δ5 cells were intravenously injected with 1 mg kg^{-1} body weight of EGF-β-gal (Figure 5a). Four hours later, Galacto-Light Plus, bioluminescence β-gal substrate, was stereotactically injected into the brain cavity through the original burr-hole used to implant the tumors. Targeted-β-gal crossed the BBTB as measured and quantified by bioluminescence imaging in living mice (Figure 5b). Little to no

DOI: 10.1021/bc500597y
Bioconjugate Chem. 2015, 26, 660−668

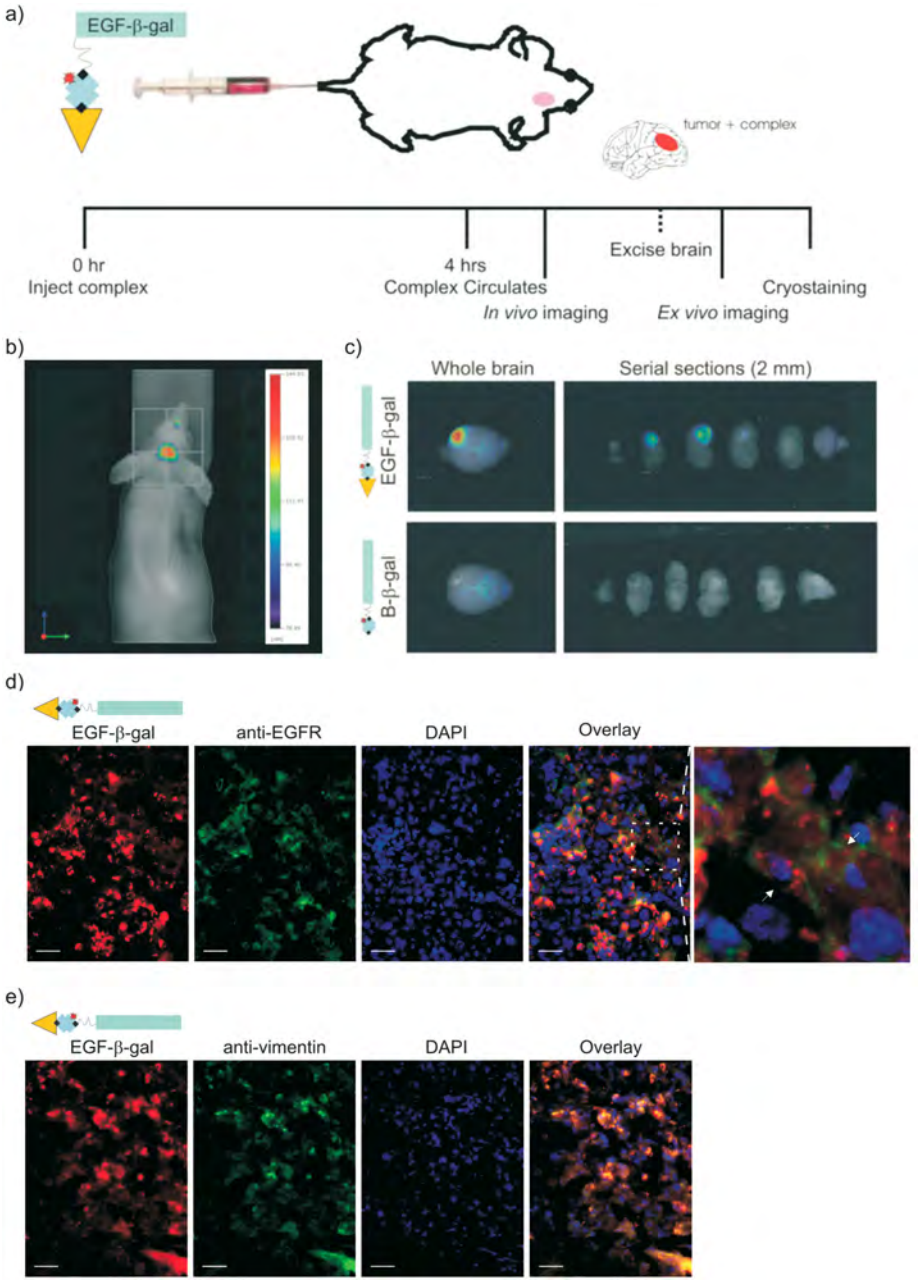

Figure 3. Fluorescence imaging of targeted-β-galactosidase complex in orthotopic brain tumors. (a) Flow chart of in vivo imaging for mice intravenously administered EGF-β-gal. FMT of a mouse with (b) orthotopic GBM administered EGF-β-gal (1 mg kg^{-1} body weight) intravenously. The color bar represents the concentration (nM) of activated probe. (c) Mice containing implanted gliomas were administered EGF-β-gal or B-β-gal intravenously. The brains were then excised and imaged using in vivo multispectral fluorescence. (d,e) Excised brains were cryosectioned and immunostained with anti-EGFR and anti-vimentin to demonstrate uptake localization of EGF-β-gal.

bioluminescence was observed in sham treated mice (PBS). Stereotactic injection was utilized, in this case, as the substrate in our hands was found to be toxic upon systemic injection. Development of less toxic β-gal-activatable substrates is underway.

DISCUSSION

β-Gal is a very robust enzyme whose activity is maintained under a variety of different conditions, including tissue fixation, which is why it has been so widely selected for decades by molecular biologists as a tool to measure gene expression in several different settings. Many reporter substrates exist for this enzyme, but most are limited to histological or in vitro use. Recently, several investigators have demonstrated the use of β-gal as a marker for noninvasive imaging of gene expression using MRI,[15,28] bioluminescence,[4,26] and NIRF imaging.[3] Although each technique is unique in its derivation and application, all share the characteristic of requiring genetic manipulation of target cells to allow in vivo measurement of β-gal activity. For the methods of both Mason and Weissleder, β-gal activity is directly measured after it is expressed in the target cells, which then can activate a substrate to generate bioluminescence or fluorescence in vivo, respectively. In another iteration, Meade and co-workers use a caged gadolinium, which is conformationally exposed after β-gal cleavage, to generate signal enhancement for MRI.[15] In these studies, transfection of a plasmid containing the 3000 bp β-gal

DOI: 10.1021/bc500597y
Bioconjugate Chem. 2015, 26, 660−668

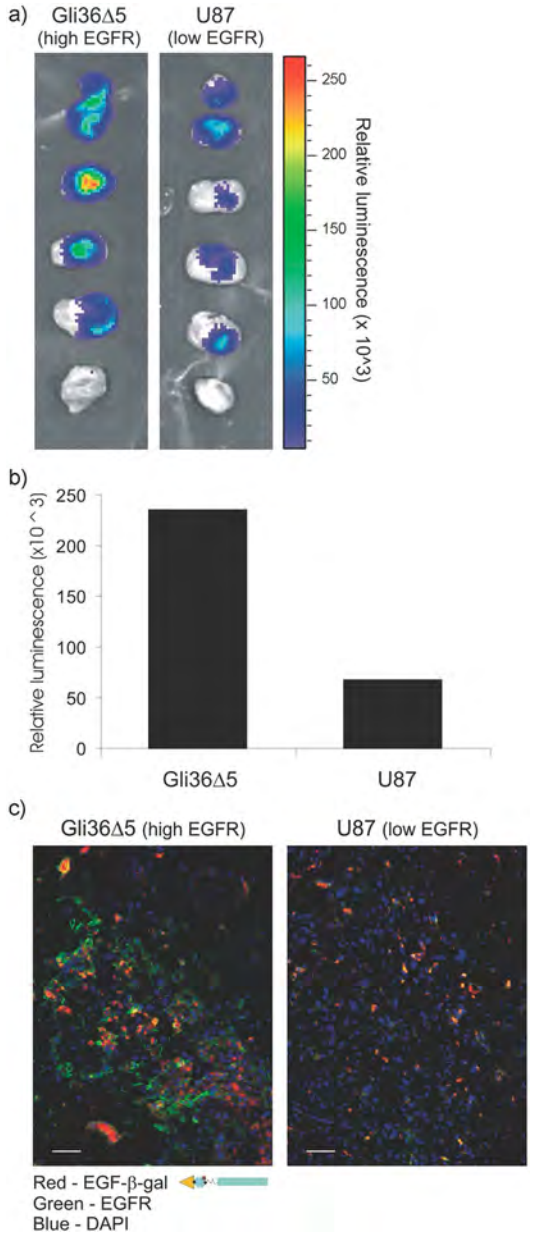

Figure 4. Ex vivo bioluminescence imaging of targeted-β-galactosidase complex. (a) Mice containing implanted gliomas from Gli36Δ5 or U87 cells were administered EGF-β-gal (1 mg kg^{-1} body weight) intravenously. The brains were then removed and covered in Galacto-Light Plus, a bioluminescence substrate for β-gal. (b) Relative luminescence (photons per area per second) was calculated from each 2 mm brain slice and plotted. (c) Differential levels of EGFR expression were validated by immunostaining with anti-EGFR of cryosections from EGF-β-gal administered, tumor-containing brain.

sequence was required to generate ~88−352 copies of the plasmid per cell at the 100 000-cell stage. For MRI, this required that many millions of β-gal enzymes needed to be expressed in the *Xenopus* embryo of 1 mm diameter to achieve a significant enhancement of the T_1 signal.

Blau and co-workers use β-gal enzyme to activate a caged luciferase substrate measuring β-gal activity by the "un-caging" of the substrate, which is then used by luciferase to generate a signal.[4] In this paradigm, the target tissue or cells need to express luciferase, but it is not required that they express β-gal. Interestingly, they demonstrated that exogenous β-gal could be administered as an antibody conjugate to an animal, targeting it to cells that express luciferase. After administration of the caged luciferase, Lugal, the compound is converted in situ to luciferin, which enters the cells and serves as a substrate for luciferase expressed within the cells.[4]

We have developed a technology for noninvasive assessment by β-gal, which does not require genetic engineering of an animal model expressing β-gal. In our system, an engineered β-gal enzyme is purified from *E. coli*. Because of a biotinylation element contained within the N-terminal end of the enzyme,[16] the protein is able to complex with SA and another biotinylated ligand. This complex can be directly injected into mice bearing a brain tumor and accumulates within tumors dependent on the number of surface proteins (targets) that the tumor cells express. Injection of a β-gal bioluminescent substrate, such as Galacto-Light Plus, allows quantitative readout of β-gal activity.

The use of an injectable β-gal complex eliminates many of the restrictions for previous applications to exploit β-gal as a biomarker (i.e., genetic manipulation of target tissue) and moves β-gal into the realm of an imaging tool that can be used to identify the location of biomarkers without any a priori knowledge of the location of their expression. A combination of both fluorescent marker and enzymatic reporter (bioluminescence) in one complex could facilitate the study of the intended target at different spatial resolution and intensity scales. Multiple approaches could be used to follow a molecular target or pathway. Additionally, the utilization of β-gal, as described, provides an opportunity to begin to utilize multiple receptors expressed on the same cell surface to drive signal generation. In this scenario, β-gal would be targeted to the cell surface using one biomarker and an imageable substrate targeted to a different receptor on the cell surface allowing for activation by localized β-gal. One interesting avenue is the development of activatable MR contrast agents that could be directed to the cell surface for β-gal activation that would allow for high-resolution imaging of targeted tissues. Further, this approach potentially increases the sensitivity for such detection as the use of a bioluminescence substrate eliminates autofluorescence background, thereby reducing signal-to-noise (SNR) for many fluorescence-based noninvasive imaging approaches. Typically, fluorescence is coupled with bioluminescence to provide an additional means to gain more histological and cellular positional information.

The studies described here also potentially provide another approach to novel antibody-directed enzyme pro-drug therapy (ADEPT) approach to chemotherapy for cancer.[29−32] In the case of ADEPT, β-gal is utilized to activate a pro-drug therapy in a two-step approach much like that proposed in this study. In the first step, a drug-activating enzyme is targeted and expressed in tumors. In the second step, a nontoxic pro-drug, a substrate of the exogenous enzyme that is now localized to tumor tissues, is administered systemically. The result is that a systemically administered pro-drug can be converted to high local concentration of an active anticancer drug in tumors by a targeted enzyme, such as β-gal. With this platform, a personalized approach to patient care can also be developed. β-gal can be targeted to a patient's cancer utilizing *any cell surface marker* identified in a genomic screen as specifically overexpressed in the particular cancer, followed by pro-drug therapy. The complexes demonstrated here provide a robust platform for the targeting of β-gal (or other enzymes) to any number of different biomarkers using endogenous ligands, small molecule ligands, as well as antibodies. This potentially provides a means to target cell surface proteins for which no antibodies exist or for which

DOI: 10.1021/bc500597y
Bioconjugate Chem. 2015, 26, 660−668

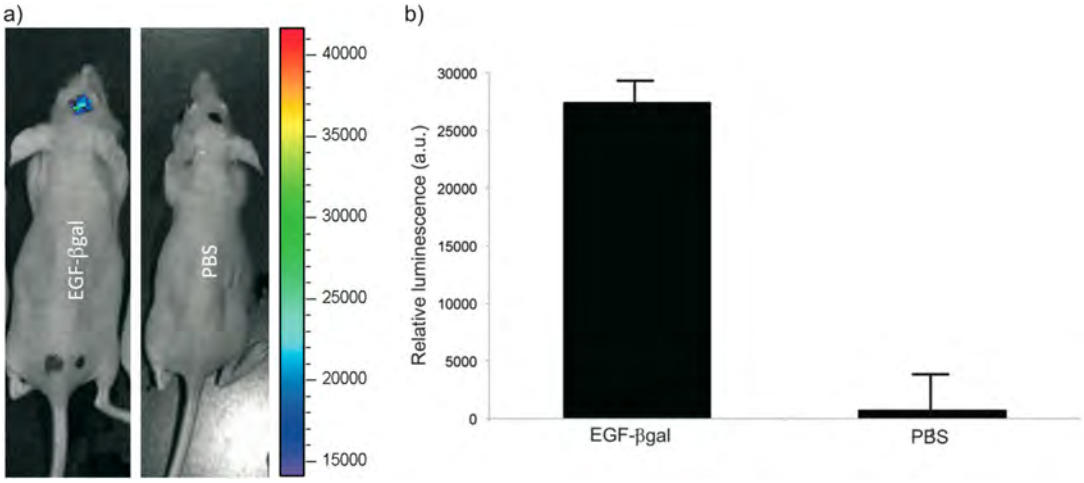

Figure 5. Bioluminescence imaging of targeted-β-galactosidase complex in orthotopic brain tumors. Mice injected intravenously with either EGF-β-gal (1 mg kg^{-1} body weight) or sham saline were imaged after stereotactic administration of Galacto-Light Plus. Scale bar represents relative luminescence.

conjugation chemistries destroy enzymatic activity of the pro-drug-activating enzyme. Indeed for β-gal, several pro-drug substrates do exist, which, when activated, generate toxicity for cancer cells both in vitro and in vivo.[32−35]

In summary, we have developed a novel conjugation of engineered β-gal that allows for rapid purification and complex formation of the enzyme with virtually any biotinylated ligand or antibody and application of the complex to cells, both in vitro and in vivo allowing for rapid identification of target expression. The direct approach of administering targeted β-gal complexes combined with the use of bioluminescent substrate eliminates the need for genetic manipulation of the target tissue and rapid readout of target expression. While demonstrated for β-gal, there is no reason that this approach cannot be used for other enzymes and it has the potential to also be used to activate pro-drugs once existence of the targeted biomarker is confirmed by imaging.

EXPERIMENTAL SECTION

β-Galactosidase Complex Creation, Propagation, and Purification. DNA encoding the full-length β-gal from the pSV-β-gal plasmid (Promega; Madison, WI) was amplified by PCR using plasmid template and primers that introduce flanking restriction enzyme sequences. The PCR product was ligated into a pHAT10 vector (Clontech; Mountain View, CA) containing a suitable antibiotic selectable marker for bacterial propagation. The resulting coding sequence, consisting of the His-tag and full-length β-gal, was excised from the vector and inserted into the pAN4 vector (Avidity; Aurora, CO). The pAN4 vector was used to express a single N-terminal biotin−protein fusion.

Luria−Bertani (LB) broth (5 mL) containing ampicillin (50 mg mL^{-1}) was inoculated with a bacterial scrape (~25 mL) containing full-length β-gal plasmid and allowed to grow overnight (18−20 h) in an incubator orbital shaker at 37 °C. Following the growth period, LB broth (1 L) with ampicillin (50 mg mL^{-1}) was inoculated with the 5 mL overnight growth and placed in the incubator/orbital shaker at 37 °C until an absorbance of 0.4 was observed at 600 nm (5.5 h). The bacterial culture was then induced with 1 mM IPTG. The IPTG-induced culture was grown in an incubator/orbital shaker at 37 °C until a reading between 0.8 and 1.0 was observed at absorbance 600 nm (6 h). Upon completion, the cells were pelleted and the supernatant discarded. The cell pellet was lysed with lysozyme at room temperature for 20 min and then stored at −80 °C until purification.

β-Gal was purified from contaminating bacterial cell degradation products and other particles using affinity chromatography. The whole cell lysate was thawed at 37 °C, sonicated, and centrifuged. The lysate was passed over a nickel Talon affinity column (Clontech; Mountain View, CA) using gravity flow. The column was washed twice with extraction buffer [50 mM $NaHPO_4$, pH 7; 300 mM NaCl in ddH_2O]. The His-tagged protein was eluted off the column in 0.5 mL fractions with elution buffer [0.15 M imidazole in extraction buffer]. Each fraction was analyzed for the presence and concentration of purified protein using standard protein analysis (Bio Rad DC Protein Assay kit; Bio Rad; Hercules, CA) and immunoblot analysis with anti-His (Upstate, Billerica, MA) and HRP-conjugated SA (Chemicon; Temecula, CA). Fractions containing the desired protein were combined, dialyzed against PBS, and stored at 4 °C.

Targeted-Reporter Complex Assay for Live Cells. Biotinylated EGF for the EGFR was linked to biotinylated β-gal using fluorophore-conjugated SA. Ligand, linker, and reporter fragment were mixed in a molar ratio 1:1:3 at room temperature for 1 h. Excess D-biotin was added to block any remaining unbound SA sites. In the case of control assays, untargeted reporter complex was prepared with D-biotin, in place of the ligand, mixed with linker and reporter fragment in a molar ration 1:1:3. The ligand-complex was then diluted to 500 mL with cell feeding media (DMEM, 10% fetal bovine serum, 1% penicillin−streptomycin) and added directly to coverslips seeded with cells overexpressing human EGFR. Cells were incubated with EGF ligand-complex for 1 h at 37 °C. The cells were then fixed with 4% paraformaldehyde, rinsed with X-gal wash buffer, and stained overnight at 37 °C with 1 mg mL^{-1} X-gal (5-bromo-4-chloro-3-indolyl-β-D-galactopyranoside; Sigma; St Louis, MO, USA) in 5 mM $K_3Fe(CN)_6$, 5 mM $K_4Fe(CN)_6$, and 2 mM $MgCl_2$ in PBS. Cells were rinsed twice with PBS for 5 min. Images were captured by a Retiga EXi camera connected to a Leica DM4000 B upright microscope (Leica Microsystems; Wetzlar, Germany).

Immunofluorescence Staining of Targeted-Reporter Complex. Biotinylated EGF was linked to biotinylated β-gal using fluorophore-conjugated SA. Ligand, linker, and reporter fragment were mixed in a molar ratio 1:1:3 at room temperature for 1 h. Excess D-biotin was added to block any remaining

DOI: 10.1021/bc500597y
Bioconjugate Chem. 2015, 26, 660−668

unbound SA sites. In the case of control assays, untargeted reporter complex was prepared with D-biotin, in place of the ligand, mixed with linker and reporter fragment in a molar ration 1:1:3. The ligand-complex was then diluted to 500 mL with cell feeding media (DMEM, 10% fetal bovine serum, 1% penicillin−streptomycin) and added directly to coverslips seeded with cells overexpressing human EGFR. Cells were incubated with EGF ligand-complex for 1 h at 37 °C. For competition assays, cells were incubated with a combination of EGF-β-gal and either 200 nM or 1000 nM full-length EGF for 4 h. The cells were then fixed with 4% paraformaldehyde, rinsed with PBS, and blocked with 1% host serum for 30 min at room temperature. Coverslips were incubated with primary antibody at room temperature for 2 h. Antibodies used were mouse anti-EGFR (1:100 dilution; Dako; Carpinteria, CA), mouse anti-EEA1 (1:100 dilution; Cell Signaling Technology; Danvers, MA), rabbit anti-Lamp2 (1:500 dilution; Sigma-Aldrich; St. Louis, MO), and rabbit anti-Rab9 (1:500 dilution; Sigma-Aldrich; St. Louis, MO). The coverslips were then rinsed with PBS and counterstained with 2-(4-amidinophenyl)-6-indolecarbamidine dihydrochloride (DAPI) for 10 min at room temperature to visualize the nuclei. After a final rinse with PBS, the coverslips were mounted using Fluor-Mount aqueous media, sealed with nail polish, and observed using epifluorescence microscopy. Relative fluorescence intensities were calculated using *ImageJ* software (NIH, MD).

Orthotopic Brain Tumor Implantation. Athymic nude female mice (*nu/nu*, 6−8 weeks at time of surgery) were bred and maintained at the Animal Resource Center at Case Western Reserve University. All procedures were performed aseptically according to Institutional Animal Care and Use Committee (IACUC) approved protocols. For brain tumor implants, mice were anesthetized by intraperitoneal injection of 50 mg kg^{-1} ketamine:xylazine and fitted into a stereotaxic rodent frame (David Kopf Instruments; Tujunga, CA). A small incision was made just lateral to midline to expose the bregma suture. A small (1.0 mm) burr hole was drilled at AP = +1, ML = −2.5 from bregma. Glioblastoma cells were slowly deposited at a rate of 1 μL per minute in the right striatum at a depth of −3 mm from dura with a 10 mL Hamilton syringe (26G blunt needle; Fisher Scientific; Waltham, MA). The needle was slowly withdrawn and the incision was closed with 2−3 sutures. For flank tumor implants, mice were anesthetized with inhaled isofluorane:oxygen for immobilization. The Matrigel:cell mixture was loaded into a 1 mL syringe fitted with a 26-gauge needle and kept on ice. The mixture was injected subcutaneously in the right flank region of the mouse. The needle was withdrawn and the animal was returned to the cage for daily monitoring.

Small Animal in Vivo Fluorescence Imaging. EGFR-targeted β-gal (EGF-β-gal) or nontargeted β-gal (B-β-gal) (1 mg kg^{-1} body weight) was intravenously injected into mice harboring orthotopic brain tumors (N = 3 for each group). After 4 h of circulation, fluorescent molecular tomographic images were obtained using FMT2500 (PerkinElmer; Waltham, MA) and three-dimensional reconstructions of fluorescent signals were acquired using the accompanying software *TrueQuant*. Quantitative fluorescent signals for Alexa 647 were calibrated per manufacturer's instructions using the 635-channel. Region of interest (ROI) was assigned based on the precise placement of cells during implantation at 3−4 mm into the brain. ROI was corroborated with fluorescent signals from ex vivo imaging.

Fluorescent multispectral images (647 nm) were obtained using the Maestro In Vivo Imaging System (CRi, Inc.; Woburn, MA) after the brains were removed. A band-pass filter appropriate for the Cy5 (yellow filter set, Ex 575−605 nm, Em 645; acquisition settings 630−850) was used for emission and excitation light, respectively. The tunable filter was automatically stepped in 10 nm increments while the camera captured images at a constant exposure of 1000 ms. The brains were then serially sectioned and reimaged to more precisely identify the tumor region. To compare signal intensities, ROI were selected over the entire treated area (tumor or nontumor) and the change in fluorescence signal over baseline was determined. The spectral fluorescent images consisting of autofluorescence spectra and imaging probe were captured and unmixed based on their spectral patterns using commercially available software (*Maestro* software v 2.4.0; CRi, Inc.; Woburn, MA). Spectral libraries were generated by assigning spectral peaks to the tissue background fluorescence, background from the imaging stage, and probe within tumor at maximal activation. Total signal in the ROI in photons measured at the surface of the brain was divided by the area in order to compare between animals and imaging experiments.

Small Animal in Vivo Bioluminescence Imaging. Gli36Δ5 or U87 cells were stereotactically implanted in the brains of mice and grown for 10 days as per IUCAC approved protocols. EGFR-targeted β-gal (EGF-β-gal; mice N = 5) or nontargeted β-gal (B-β-gal; mice N = 3) (1 mg kg^{-1} body weight) was intravenously injected into mice harboring orthotopic brain tumors and allowed to circulate for 4 h. Mice were anesthetized with isoflurane and the substrate mixture, Galacto-Light Plus, 1,2-dioxetane substrates (Tropix; Bedford, MA, USA) and a light-emission accelerator containing a polymeric enhancer (Accelerator-II), was stereotactically injected into the brain cavity through the original burr-hole used to implant the tumors with a 26-guage needle immediately after the 4 h circulation time. Imaging of β-gal was performed using the Xenogen IVIS 200 in vivo imaging system (Xenogen; Caliper Life Sciences; Hopkinton, MA) within 0.5 min after application. No animals died as a result of imaging or locally administered substrate treatment. Ex vivo bioluminescence imaging of isolated organs was performed immediately after euthanasia of the animals. Dissected brains were placed on a sheet of black background and imaged with IVIS 200. Luminescence for β-gal was determined 3 min after the topical addition of 100 mL Galacto-Light Plus reagent and Accelerator-II. Relative luminescence was quantitated by creating a ROI over the brain tumor and expressed as photons s^{-1} cm^{-2}. To standardize the data, light emission was quantified from the same surface area for each brain. Corresponding gray-scale photographs and color luminescence images were superimposed and analyzed using *Living Image* analysis software v 3.1 (Xenogen). The brains were then fixed in 4% paraformaldehyde, cryo-preserved in 30% sucrose, and frozen in optimum cutting temperature compound (OCT) for cryosectioning (Leica CM3050S). Sections were collected serially at 10 or 25 mm cut directly on to slides and stored at −80 °C until immunohistochemical staining. Cryosections of the tumor region were then counterstained with DAPI, mouse anti-EGFR (1:100 dilution; Dako; Carpinteria, CA), or rabbit anti-vimentin (1:500 dilution; LabVision; Fremont, CA), and visualized using fluorescence microscopy.

DOI: 10.1021/bc500597y
Bioconjugate Chem. 2015, 26, 660−668

AUTHOR INFORMATION

Corresponding Author

*E-mail: broomea@musc.edu. Office: 1-843-876-2481. Fax: 1-843-876-2469.

Author Contributions

The manuscript was written through contributions of all authors. All authors have given approval to the final version of the manuscript.

Notes

The authors declare no competing financial interest.

ACKNOWLEDGMENTS

This work was supported by the National Foundation for Cancer Research (to J.P.B.) and a fellowship award (to A.M.B.). The project described was also supported by Grant Number K01EB006910 (to A.M.B.) from the National Institute of Biomedical Imaging and Bioengineering and by the Department of Defense Peer Reviewed Cancer Research Program Idea Award Grant Number W81XWH-11-1-0386 (to A.M.B.). The content and views are solely the responsibility of the authors and do not necessarily represent the official views of the National Institute of Biomedical Imaging and Bioengineering or the National Institutes of Health or the US Army or the Department of Defense.

ABBREVIATIONS

ADEPT, antibody-directed enzyme pro-drug therapy; B, biotin; β-gal, beta-galactosidase; BBB, blood brain barrier; BBTB, blood brain tumor barrier; DAPI, 4′,6-diamidino-2-phenylindole; DDAGO, 9*H*-(1,3-dichloro-9,9-dimethylacridin-2-one-7-yl) β-D-galactopyranoside; EGF, epidermal growth factor; EGFR, epidermal growth factor receptor; GBM, glioblastoma multiform; IUCAC, Institutional Use and Care Animal Committee; MRI, magnetic resonance imaging; NIR, near-infrared; NIRF, near-infrared fluorescence; PBS, phosphate buffered saline; ROI, region of interest; SA, streptavidin; X-gal, 5-bromo-4-chloro-3-indolyl-β-D-galactoside; SNR, signal-to-noise ratio

REFERENCES

(1) Flanagan, W. M., and Wagner, E. K. (1987) A bi-functional reporter plasmid for the simultaneous transient expression assay of two herpes simplex virus promoters. *Virus Genes 1* (1), 61−71.

(2) Jain, C. (1993) New improved lacZ gene fusion vectors. *Gene 133* (1), 99−102.

(3) Tung, C. H., Zeng, Q., Shah, K., Kim, D. E., Schellingerhout, D., and Weissleder, R. (2004) In vivo imaging of beta-galactosidase activity using far red fluorescent switch. *Cancer Res. 64* (5), 1579−83.

(4) von Degenfeld, G., Wehrman, T. S., and Blau, H. M. (2009) Imaging beta-galactosidase activity in vivo using sequential reporter-enzyme luminescence. *Methods Mol. Biol. 574*, 249−59.

(5) Wehrman, T. S., von Degenfeld, G., Krutzik, P. O., Nolan, G. P., and Blau, H. M. (2006) Luminescent imaging of beta-galactosidase activity in living subjects using sequential reporter-enzyme luminescence. *Nat. Methods 3* (4), 295−301.

(6) Chen, S. H., Kuo, Y. T., Singh, G., Cheng, T. L., Su, Y. Z., Wang, T. P., Chiu, Y. Y., Lai, J. J., Chang, C. C., Jaw, T. S., Tzou, S. C., Liu, G. C., and Wang, Y. M. (2012) Development of a Gd(III)-based receptor-induced magnetization enhancement (RIME) contrast agent for beta-glucuronidase activity profiling. *Inorg. Chem. 51* (22), 12426−35.

(7) Aime, S., Gianolio, E., Terreno, E., Giovenzana, G. B., Pagliarin, R., Sisti, M., Palmisano, G., Botta, M., Lowe, M. P., and Parker, D. (2000) Ternary Gd(III)L-HSA adducts: evidence for the replacement of inner-sphere water molecules by coordinating groups of the protein. Implications for the design of contrast agents for MRI. *J. Biol. Inorg. Chem. 5* (4), 488−97.

(8) Hanaoka, K., Kikuchi, K., Terai, T., Komatsu, T., and Nagano, T. (2008) A Gd3+-based magnetic resonance imaging contrast agent sensitive to beta-galactosidase activity utilizing a receptor-induced magnetization enhancement (RIME) phenomenon. *Chemistry 14* (3), 987−95.

(9) Breckwoldt, M. O., Chen, J. W., Stangenberg, L., Aikawa, E., Rodriguez, E., Qiu, S., Moskowitz, M. A., and Weissleder, R. (2008) Tracking the inflammatory response in stroke in vivo by sensing the enzyme myeloperoxidase. *Proc. Natl. Acad. Sci. U. S. A. 105* (47), 18584−9.

(10) Gulaka, P. K., Rojas-Quijano, F., Kovacs, Z., Mason, R. P., Sherry, A. D., and Kodibagkar, V. D. (2014) GdDO3NI, a nitroimidazole-based T1MRI contrast agent for imaging tumor hypoxia in vivo. *J. Biol. Inorg. Chem. 19* (2), 271−9.

(11) Querol, M., Chen, J. W., Weissleder, R., and Bogdanov, A., Jr. (2005) DTPA-bisamide-based MR sensor agents for peroxidase imaging. *Org. Lett. 7* (9), 1719−22.

(12) Iwaki, S., Hanaoka, K., Piao, W., Komatsu, T., Ueno, T., Terai, T., and Nagano, T. (2012) Development of hypoxia-sensitive Gd^{3+}-based MRI contrast agents. *Bioorg. Med. Chem. Lett. 22* (8), 2798−802.

(13) Giardiello, M., Lowe, M. P., and Botta, M. (2007) An esterase-activated magnetic resonance contrast agent. *Chem. Commun. (Cambridge) 39*, 4044−6.

(14) Touti, F., Maurin, P., and Hasserodt, J. (2013) Magnetogenesis under physiological conditions with probes that report on (bio-)chemical stimuli. *Angew. Chem., Int. Ed. 52* (17), 4654−8.

(15) Urbanczyk-Pearson, L. M., and Meade, T. J. (2008) Preparation of magnetic resonance contrast agents activated by beta-galactosidase. *Nat. Protoc. 3* (3), 341−50.

(16) Broome, A. M., Bhavsar, N., Ramamurthy, G., Newton, G., and Basilion, J. P. (2010) Expanding the utility of beta-galactosidase complementation: piece by piece. *Mol. Pharmaceutics 7* (1), 60−74.

(17) Cohen, A. L., and Colman, H. (2015) Glioma biology and molecular markers. *Cancer Treat Res. 163*, 15−30.

(18) Faulkner, C., Palmer, A., Williams, H., Wragg, C., Haynes, H. R., White, P., DeSouza, R. M., Williams, M., Hopkins, K., and Kurian, K. M. (2014) EGFR and EGFRvIII analysis in glioblastoma as therapeutic biomarkers. *Br. J. Neurosurg.*, 1−7.

(19) Hatanpaa, K. J., Burma, S., Zhao, D., and Habib, A. A. (2010) Epidermal growth factor receptor in glioma: signal transduction, neuropathology, imaging, and radioresistance. *Neoplasia 12* (9), 675−84.

(20) Hegi, M. E., Rajakannu, P., and Weller, M. (2012) Epidermal growth factor receptor: a re-emerging target in glioblastoma. *Curr. Opin. Neurol. 25* (6), 774−9.

(21) Talasila, K. M., Soentgerath, A., Euskirchen, P., Rosland, G. V., Wang, J., Huszthy, P. C., Prestegarden, L., Skaftnesmo, K. O., Sakariassen, P. O., Eskilsson, E., Stieber, D., Keunen, O., Brekka, N., Moen, I., Nigro, J. M., Vintermyr, O. K., Lund-Johansen, M., Niclou, S., Mork, S. J., Enger, P. O., Bjerkvig, R., and Miletic, H. (2013) EGFR wild-type amplification and activation promote invasion and development of glioblastoma independent of angiogenesis. *Acta Neuropathol. 125* (5), 683−98.

(22) Chakravarti, A., Chakladar, A., Delaney, M. A., Latham, D. E., and Loeffler, J. S. (2002) The epidermal growth factor receptor pathway mediates resistance to sequential administration of radiation and chemotherapy in primary human glioblastoma cells in a RAS-dependent manner. *Cancer Res. 62* (15), 4307−15.

(23) Nakamura, J. L. (2007) The epidermal growth factor receptor in malignant gliomas: pathogenesis and therapeutic implications. *Expert Opin. Ther. Targets 11* (4), 463−72.

(24) Weppler, S. A., Li, Y., Dubois, L., Lieuwes, N., Jutten, B., Lambin, P., Wouters, B. G., and Lammering, G. (2007) Expression of EGFR variant vIII promotes both radiation resistance and hypoxia tolerance. *Radiother. Oncol. 83* (3), 333−9.

(25) Li, Z., Zhao, R., Wu, X., Sun, Y., Yao, M., Li, J., Xu, Y., and Gu, J. (2005) Identification and characterization of a novel peptide ligand of

DOI: 10.1021/bc500597y
Bioconjugate Chem. 2015, 26, 660−668

epidermal growth factor receptor for targeted delivery of therapeutics. *FASEB J. 19* (14), 1978−85.
(26) Liu, L., and Mason, R. P. (2010) Imaging beta-galactosidase activity in human tumor xenografts and transgenic mice using a chemiluminescent substrate. *PLoS One 5* (8), e12024.
(27) Agnes, R. S., Broome, A. M., Wang, J., Verma, A., Lavik, K., and Basilion, J. P. (2012) An optical probe for noninvasive molecular imaging of orthotopic brain tumors overexpressing epidermal growth factor receptor. *Mol. Cancer Ther 11* (10), 2202−11.
(28) Urbanczyk-Pearson, L. M., Femia, F. J., Smith, J., Parigi, G., Duimstra, J. A., Eckermann, A. L., Luchinat, C., and Meade, T. J. (2008) Mechanistic investigation of β-galactosidase-activated MR contrast agents. *Inorg. Chem. 47* (1), 56−68.
(29) Bagshawe, K. D. (1987) Antibody directed enzymes revive anti-cancer prodrugs concept. *Br. J. Cancer 56* (5), 531−2.
(30) Bagshawe, K. D. (2006) Antibody-directed enzyme prodrug therapy (ADEPT) for cancer. *Expert Rev. Anticancer Ther. 6* (10), 1421−31.
(31) Senter, P. D., and Springer, C. J. (2001) Selective activation of anticancer prodrugs by monoclonal antibody-enzyme conjugates. *Adv. Drug Delivery Rev. 53* (3), 247−64.
(32) Legigan, T., Clarhaut, J., Tranoy-Opalinski, I., Monvoisin, A., Renoux, B., Thomas, M., Le Pape, A., Lerondel, S., and Papot, S. (2012) The first generation of beta-galactosidase-responsive prodrugs designed for the selective treatment of solid tumors in prodrug monotherapy. *Angew. Chem., Int. Ed. 51* (46), 11606−10.
(33) Farquhar, D., Pan, B. F., Sakurai, M., Ghosh, A., Mullen, C. A., and Nelson, J. A. (2002) Suicide gene therapy using E. coli beta-galactosidase. *Cancer Chemother. Pharmacol. 50* (1), 65−70.
(34) Legigan, T., Clarhaut, J., Renoux, B., Tranoy-Opalinski, I., Monvoisin, A., Berjeaud, J. M., Guilhot, F., and Papot, S. (2012) Synthesis and antitumor efficacy of a β-glucuronidase-responsive albumin-binding prodrug of doxorubicin. *J. Med. Chem. 55* (9), 4516−20.
(35) Tietze, L. F., and Krewer, B. (2009) Antibody-directed enzyme prodrug therapy: a promising approach for a selective treatment of cancer based on prodrugs and monoclonal antibodies. *Chem. Biol. Drug Des. 74* (3), 205−11.

DOI: 10.1021/bc500597y
Bioconjugate Chem. 2015, 26, 660−668